UNIVERSITY OF OSLO
Department of Physics

Diffraction Effects in Sonar Array

Master Thesis in Electronics and Computer Technology

Mohammad Khidash Kiyani

September 2014

Diffraction effects in sonar array

Mohammad Khidash Kiyani

Friday 5th September, 2014

Abstract

Humans can localize a sound source with the help of three effects, Head Related Transfer Function (HRTF), Interaural Time Difference (ITD) and Interaural Level Difference (ILD). With help of these three effects humans can sense where in the space the signal is coming from. The space can be described by three planes: vertical-, horizontal- and median plane. Sound localization is described by three dimensions: azimuth angle, elevation angle and distance or velocity detection for static or moving source.

Diffraction of sound by human head is described by the diffraction formula. The sound is diffracted by the human head if the dimension of the head is smaller compared to $2\lambda/3$.

Sonar means Sound Navigation and Ranging, and has its roots from as early as the beginning of World War I. Sonar technology was actively used under World War I and World War II, and had an increase of interest among the scientists after this period. Sound is pressure perturbations that travels as a wave spreads spherically or cylindrically in the water by describing the decrease of the signal. Sound propagation is affected by absorption, refraction, reflection and scattering. There are three types of sonar equations described in this thesis, *the active sonar equation for noise background*, *the active sonar equation for reverberation background* and *the passive sonar equation*.

In sonar the distance to the sound source is calculated by the travel time and the sound velocity of the incoming sound wave. Sound velocity in water is divided into four different regions and is temperature dependent. For circular and spherical arrays, (just like the human head), the sound wave travels direct to the receiver as long as the elements has a "direct" path to the receiver. Otherwise the sound signal is diffracted and travels along the surface of the transducer (with different sound velocity from as in water) until it has a "direct" path to the receiver. This has its limitations, and for some rotational angle on the transducer the sound wave is not possible to detect. This angle limitation depends on the normalized frequency $\mu = ka = \frac{2\pi a}{\lambda}$ value. where a is radius of the circular transducer. In this thesis I'm going to study at which rotational angle α the signal disappears when sending a sound signal pulse with frequency $f = 100kHz$ and a normalized frequency $\mu = 25$, and compare it with human listening.

Contents

List of Figures

List of Tables

Acronyms

HRTF Head related transfer function

ITD Interaural time difference

ILD Interaural level difference

IID Interaural intensity difference

IPD Interaural phase difference

MAMA Minimum audible movement angle

Sonar Sound Navigation and Ranging

Radar Radio Detection And Ranging

CW Continuous wave

Preface

This master thesis was carried out at the Depertment of Physics, Faculty of Mathematics and Natural Science, University of Oslo (UiO) in the period January 2013 - September 2014. The thesis is for the grade Master of Science in Electronics and Computer Technology and contributes 60 credits.

Executing the master thesis has been both interesting and challenging. This project contributes a great experience in life. Since I was one of two first students to work on this tank system, it made it extra challenging and interesting.

First of all, I want to thank my supervisor, Professor Sverre Holm, for motivating me to work on this project and for providing me all the valuable and necessary guidance and inspiration. Secondly I want to thank my co-student, Asle Tangen, who worked with me on the tank from the very beginning of my master thesis.

A special thanks goes to senior engineer, Svein Bøe, who helped us understanding the simulation process in the tank. I also want to thank professor, Andreas Austeng and the whole group of DSB at UiO. You were always supporting and helpful, and it was a pleasure working with you guys. A special gratitude I give to Kongsberg Maritime AS, who allowed us to borrow the transducer as well as the tube for the project. Without your help this project couldn't have started.

In the end, I want to thank all my friends and family for all their motivation, support and patience throughout my study.

Mohammad Khidash Kiyani
Oslo, 5th September 2014

Part I

Introduction

Chapter 1

Introduction

1.1 Motivation

Humans can sense the direction of the sound source, no matter where the signal is coming from. Human ear's can be considered as sensors or antennas, who detects the sound signal and determines the direction of the sound source with help of the sound level and the time delay between both ears.

Can a circular or spherical sonar array behave like a human head? How does the sound diffract around this array? Is it possible to detect signals coming from behind, or is it possible to receive the signal transmitted from circular or spherical transducer with the element 180° from the receiver? Can this strengthen the theory of fish finding in water?

1.2 Thesis outline

Chapter 2 gives an introduction to human listenening. How sound is diffracted around human head, and how humans are able to localize sound sources are discussed in this chapter.

Chapter 3 gives an introduction to sonar. Starting with some history, some basic physics and then going through how sound propagates in water.

Chapter 4 describes the sonar equation. Discussing different parameters in the equation as well as describing the equation for three scenarios.

Chapter 5 gives some background information about the experiment. I'll go through every instrument/equipment used in the experiment as well as illustrating how the simulation process is done in the tank.

Chapter 6 describes the geometry between the transducer and the hydrophone. Gives some cases for the sound propagation path to the receiver for different rotational angles.

Chapter 7 describes the pre-experiments. Experiment I is done to find the maximum and minimum values for the sound wave, and to study how transducer transmits the sound wave. Experiment II is done to calculate the sound velocity.

Chapter 8 describes the main experiments. Experiment III is done to find -3dB point of the transmitted signal, and to calculate the instrumental delay. Experiment III also calculates with help of -3dB point the effective element size on the transducer. Experiment IV is done by rotating the transducer from 85° to 275°, to check whether it is possible to receive the signal from behind. Experiment IV also calculates the sound velocity when the element doesn't have a "direct" path to the receiver.

Chapter 9 gives the conclusion for the thesis and discusses some factors which may have influenced the measured data. It also provides suggestions for future work.

Part II

Background

Chapter 2

Introduction to human listening

In this chapter I'm going to introduce how humans verify or localize sounds transmitted from a sound source anywhere in the space. How is actually sound difracted around human head? How are humans able to localize where the sound is coming from?

2.1 Sound diffraction around human ear

Before sound wave reaches the human ears, it is diffracted by the head and the diffraction causes the sound to be filtered, which is characterised by the Head related transfer function (HRTF). One part of HRTF is angle dependent sound attenuation.This is called Interaural intensity difference (IID), and Interaural level difference (ILD) when measured in dB. An example of IID is given in Figure 2.1. The other part is the angle dependent time difference of arrival of sound at both left and right ears which is because of their seperation. This is called Interaural time difference (ITD), and Interaural phase difference (IPD) when measured as the phase shift of sinusoidal tone. An example of time difference is given in the Figure 2.2. The Head Related Transfer Function is dispersive, where the phase shift increases more slowly than linearly by increasing the frequency. The phase delay decreases as the frequency increases. This is the reason why high-frequency sound waves travels faster around a human head than low-frequency sound waves.

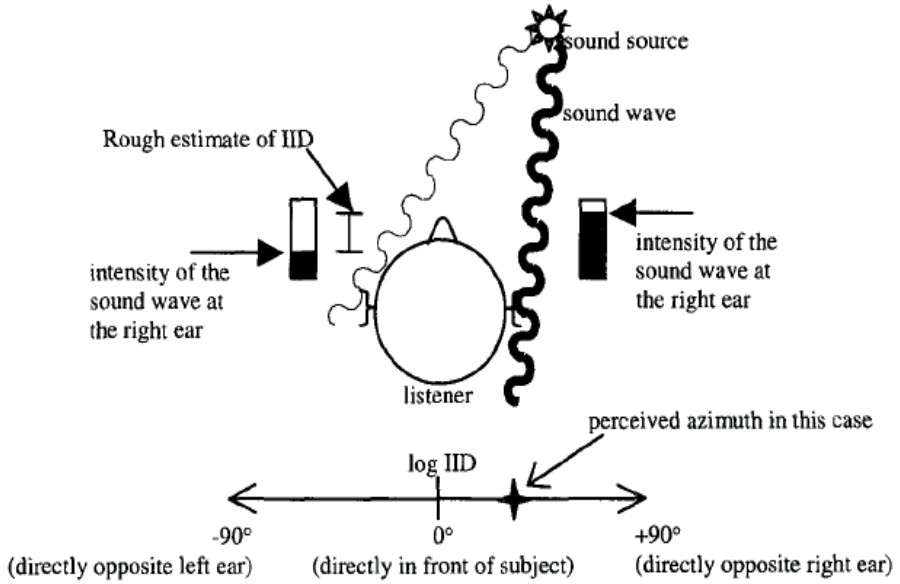

Figure 2.1: Example of IID - Figure is taken from https://cnx.org/content/m45358/latest/

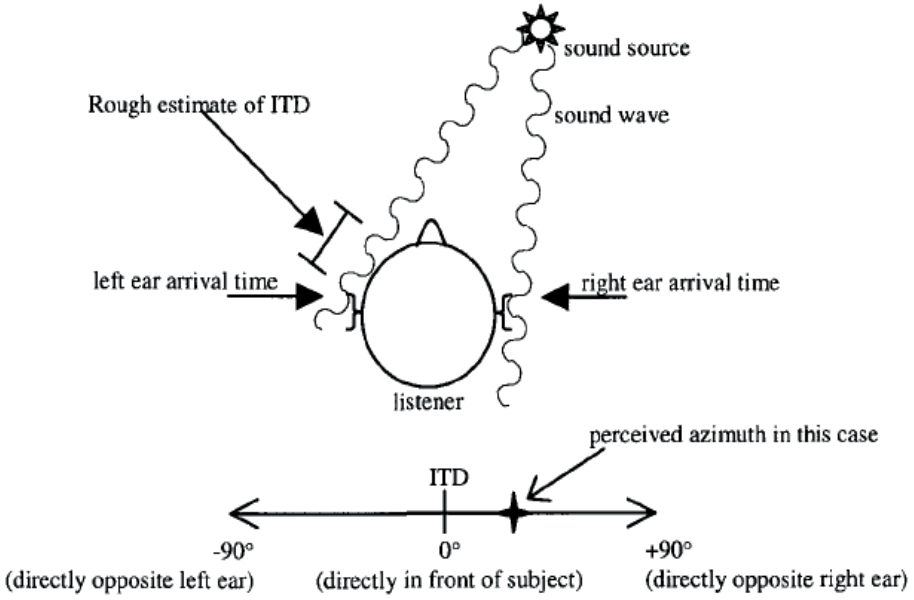

Figure 2.2: Example of ITD - Figure is taken from https://cnx.org/content/m45358/latest/

Diffraction of a sound wave occurs when dimension of the head is smaller than $2\lambda/3$, and the sound will diffract around the head and cover the potential shadow region. If the dimension is greater than $2\lambda/3$, then there will be no diffraction around the head, and we will get sound shadow region. This shown in Figure 2.3

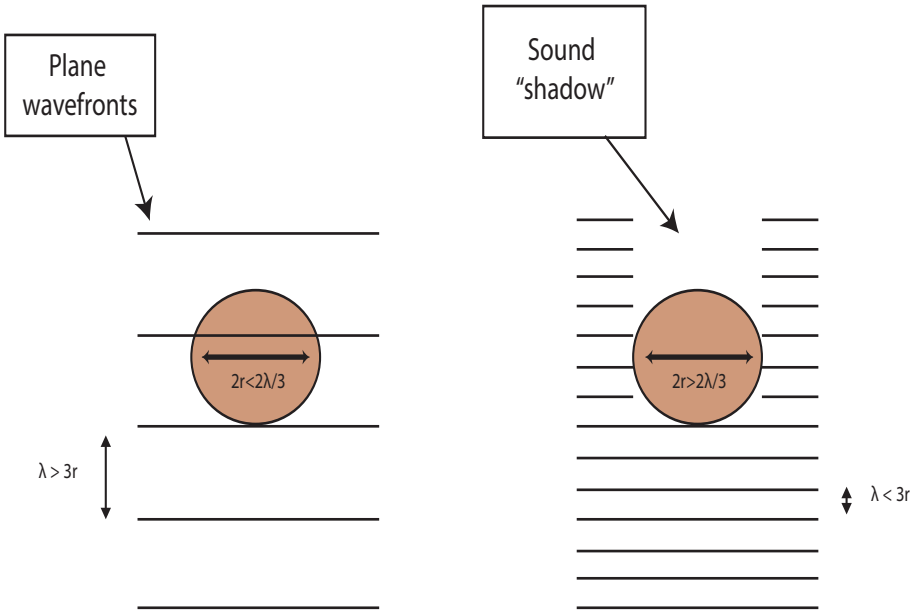

Figure 2.3: Diffraction and shadow

2.1.1 Diffraction formula

The effects of diffraction by the head, including dispersion, can be approximated by a diffraction formula for the sound pressure on the surface of a sphere as shown in Equation 2.1.

$$\left(\frac{p_i + p_s}{p_o}\right)_{r=a} = \left(\frac{1}{ka}\right)^2 \sum_{n=0}^{n_{max}} \frac{i^{n+1}(2n+1)P_n(\cos\theta)}{j'_n(ka) - iy'_n(ka)}. \tag{2.1}$$

Symbols p_i, p_s and p_o refer to incident, scattered and free-field pressures. Factor $k = \frac{2\pi}{\lambda}$, and a is the radius of the head. Function P is a Legendre polynomial. And functions j' and y' are derivatives of spherical Bessel functions and spherical Neuman functions *(Abramovitz and Stegun, 1964)*. The formula is taken from *Constan and Hartmann (2003)[**?**]*.

2.2 Sound localization

In recent years, there has been an increasing of interest in sound localizaton by human listeners. Sound localization is the process of determining the location of a sound source. There are many factors that count to localize a sound by a human brain, such as the strength or intensity of the sound, time travel, angle of incident, azimuth, elevation etc. Sound localization can be described by three-dimensional positions: the azimuth or horizontal angle, the elevation or vertical angle and the distance for static source or velocity for moving source. The three dimensions is described in Figure 2.4.

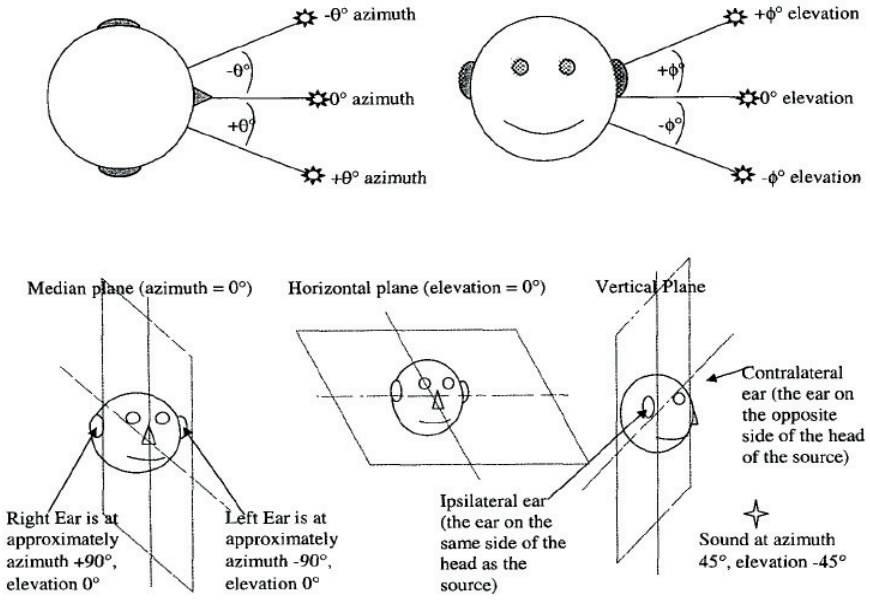

Figure 2.4: Sound localization described in 3D plane - Figure is taken from https://cnx.org/content/m45358/latest/

Time difference and intensity difference are two mechanisms that describes the sound localization process in the horizontal or azimuthal plane. Spectral cues or the HRTF are the mechanism that describes the sound localization in the vertical or elevation plane.

2.2.1 Horizontal localization

In the end of the 19th century, *Lord Rayleigh* made some important series of observations in the horizonal dimension and reported in his Segwick lecture in 1906 *(Rayleigh 1907)*. He defined localization in terms of interaural difference cues.

If a sound is coming from the side, and the listener's head is in the path of the sound traveling towards the far ear, then the far ear is shadowed and it would result in level difference. In other words, sounds coming from right has higher level difference at the right ear than the left ear. Level difference is frequency dependent and increases with increasing frequency. As mentioned earlier the amount of shadow depends on the wavelength compared with the dimension of the head.

For frequencies below 800 Hz, the dimensions of the head are smaller than the half wavelength of the sound wave. And the auditory system can determine the phase delay between both ears without confusion. Level difference is very low in this frequency range, and is therefor negligible. So for low frequencies below 800 Hz, only time difference or phase difference is used. For frequencies below 80 Hz, the phase difference between both ears

become too small to find the direction of the sound source, thus, it becomes impossible to use time difference and level difference.

For frequencies above 1600 Hz, the dimension of the head are larger than the wavelength. The level difference becomes larger, and therefor is used to find the location of the sound source in this frequency range.

For frequencies between 800Hz and 1600 Hz, there is a transition zone, where both time difference and level difference plays a part of determing the location of the sound source.

From all this it is cleared that for localizing the sound source, humans depends on time difference for low frequencies, and on level difference for high frequencies. This is often referred to as the "duplex" theory.

2.2.2 Vertical localization

If the the head and the ears are symmetrical, a stimulus presented at any location on the median plane has none interaural differences, and thus, interaural differences provides no cue to the vertical locations of sounds on the median plane. If the interaural differences, level difference or phase difference are constant, then any point off this median plane falls on a "cone of confusion".

Batteau(1967,1968) was one of the first to emphasize that the external ear, specifically the pinna (as shown in Figure 2.5), could be a source of spatial cues that might be used to localize a sound source. He meant that sound reflections within the convolutions of the pinna might produce spatial cues.

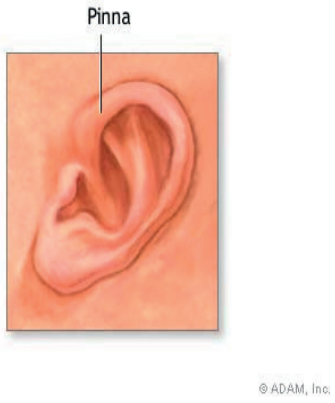

Figure 2.5: External ear or the pinna - Figure is taken from https://www.nytimes.com/imagepages/2007/08/01/health/adam/9528Pinnaofthenewbornear.html

The convolutions of the pinna creates echoes that lasts only for a few microseconds, so most theories interpret the pinna as producing changes in the spectrum of the sound source that reaches the tympanic membrance. The pinna's task is to produce multiple paths to the ear canal, including a direct path and reflection from the cavum concha of the pinna. The sum of a direct signal and a delayed version of the same signal produces a "comb-filtered" spectrum. The length of the reflected path varies with the elevation of the sound source. Patterns of spectral features associated with particular location is referred to as "spectral shape cues". They are often referred to as "pinna cues". Spectral shape cues are the major cues for vertical localization.

2.2.3 Distance perception

The ability of a human to localize the distance of a sound source is not so good. But the distance can be judged on the basis of the sound intensity at the listener's ear. In 1969, *M. B. Gardner* showed that the distance of a person speaking with a conversational tone in anechoic chamber can almost be accurately judged. The distance of the same voice transmitted from a speaker is almost determined by the sound level of the loudspeaker. Thus, familiarity to sound source seems to be an important variable. *Simpson and Stanton (1973)* have shown that head motion does not improve the judgement of the distance. In 1980, *Butler* listened to sounds over headphones and judged their apparant distance. The distance of the source increased as the low-frequency part of the spectrum increased.

But there is some evidence that states that the listener can better judge the distance of the source if the surrounding environment is not anechoic. In an ordinary room, a distant source produces sound energy that reaches the listener's ear via direct and indirect paths. Differences in the ratio of these two energies might produce differences in the quality of the source as a function of distance. This cue to source distance, however, is strongly influenced by the specific reflections of the particular listening environment, *(Middlebrooks and Green, 1991)[**?**]*.

2.2.4 Motion detection

Another consideration ragarding human listening is how humans detect sounds which are in motion or moving. In this thesis I will only refer to change in azimuth and/or elevation of the source, not the change in source distance. There is no compelling evidence for motion-sensitive systems in the auditory system. The problem is that there are two intepretations of sensitivity to source motion. One intepretation is that the auditory system is sensitive to dynamic aspects of localization cues, such as level differences or phase differences. The second intepretation is that the nervous system measures the sound source location at two distinct times and interprets a change in location as motion. This has been called the "snapshot theory". The reason why this two alternatives are difficult to resolove is because of

the fact that most studies of motion detection tend to confuse the attributes of duration, velocity, and net change in location.

Most studies have used sound sources in actual motion, some have simulated motion by systematically varying the levels of sinusoids presented from two loudspeaker. Thresholds have been measured for duration, velocity and change in location. All these thresholds, can be expressed in terms of Minimum audible movement angle (MAMA), which is the smallest net change in location of a moving stimulus that can be detected under some specified set of conditions. The MAMA shares several properties with the minimum audible angle for static sources. Some of them are: *a)* MAMAs in azimuth are smallest for stimuli around 0° azimuth and increases with increasing azimuth. *b)* MAMAs are smaller for broadband than for tonal stimuli. *c)* MAMAs are largest for a range of frequencies around 1300-2000 kHz. This applies when measured with tonal stimuli.

Chapter 3

Introduction to sonar

Sound Navigation and Ranging (Sonar) is a technique that uses sound propagation to navigate, communicate with or detect objects on or under the surface of the water, such as other vessels, *(Sonar, 2014, http://en.wikipedia.org/wiki/Sonar[**?**])*.

3.1 Sonar history

In 1490, *Leonardo Da Vinci* wrote: "If you cause your ship to stop, and place the head of a long tube in water and place the outer extremity to your ear, you will hear ships at great distance from you",*(Urick, 1983. Chapter 1, page 2)[**?**]*. From this experiment it's not possible to find the direction of the sound source. Anyway, this idea had widespread use as late as World War I. The direction could be achieved and the bearing of the target could be determined by adding a second tube between the other ear and a point in the sea separated from the first point.

As mentioned in *Urick (1983)*, perhaps the first measurements in underwater sound occured in 1827. A swiss physicist, *Daniel Colladon*, and a French methematician, *Charles Sturm*, worked together and measured the velocity of sound in Lake Geneva in Switzerland. They experimented by taking the time interval between a flash of light and the striking of a bell underwater. From this they determined the velocity of sound with some accuracy.

In the 19th century, it was a great amount of interest among scientists on underwater acustics. An invention from the 19th century is the carbon-button microphone, which is still the most sensitive hydrophone device for underwater sound. Another invention of the 19th century was the submarine bell, which was used by ships for offshore navigation. This system made it possible for ships to find their distance from a lightship. They took the time interval between the sound of the bell, which was installed above the sea surface on the lightship, and a simultaneously sent blast from a foghorn, which was installed underwater on the same lightship. This method didn't became so popular, thus, it was replaced by navigation methods involving

radio.

Echo ranging bacame very popular in the period before World War I, and in 1912, five days before the "Titanic" accident, *L.F. Richardson* did some research on echo ranging with airborne sound. A month later he used a directional projector of kilohertz-frequency sound waves and a frequency-selective receiver detuned from the transmitting frequency to compensate for doppler shift, which was caused by the moving vessel.

In 1914, it was a large amount of research on sonar for military purposes. The same year, *R.A. Fessenden* designed and built a new kind of moving coil transducer for both submarine signalling and echo ranging. It could detect an iceberg up to 2 miles away. They were installed on all United States submarines during the World War I, so they could signal each other when submerged. In France a young Russian engineer called *Constain Chilowsky*, worked together with a physicist called *Paul Langevin*. They experimented with a electrostatic projector and a carbon-button microphone placed at focus of a concav mirror. In 1916, they were able to receive echoes from bottom and from a sheet of armor plate at a distance of 200 meters. Later, in 1917 *Langevin* employed vacuum- tube amplifier, which was the first application of electronics to underwater sound equipment. For the first time in 1918, echoes was received from submarine at distances as much as 1500 meters.

At the end of World War I, *Leonardo's* air tube had been used for passive listening, and was improved by use of two tubes to take advantage of the binaural directional sense of a human observer. The MV device was mouted along the bottom of a ship on the port and starboard side. It consisted of two line arrays with 12 air tubes each. The device was steered with a special compensator. The result gave precise achievement in determining the bearing of a noisy target. Another development of the late stages of World War I was flexible line array of 12 hydrophones called the "eel". They were easy to fit on any ship and could be towed away from a noisy vessel on which it was mounted. Almost three thousand escort craft were installed with listening devices during World War I.

In 1919, after World War I, the Germans published the first scientific paper about underwater sound. In the paper it was written about bending of sound rays produced by slight temperature and salinity gradients in the sea, and their importance in determining sound ranges. This paper was unrecognized for over 60 years. The years after World War I was slow in terms of underwater sound applications for practical use. Depth sounding by ships under way was developed, and by 1925, fathometers were available commercially both in United States and Great Britain. The problem of finding a suitable projector in echo ranging was solved by resorting to magnetostrictive projectors for generating the required amount of acoustic power. Sonar received great practical impact from advances in electronics, during the period between World War I and World War II. Which made it possible

to make new technologies such as amplifying, processing, and displaying sonar information to an observer. Ultrasonic frequencies are frequencies beyond the limits of which a human ear can sense, and was used for both listening and echo ranging. The range recorder for echo ranging sonars was also developed in this period. It provided "memory"of past events and the streamlined dome to protect the transducer on a moving ship from the noisy environment. An important achievement in this period was the understanding of sound propagation in the sea. Good signals were received in the morning and bad signals or none in the evening. Bathythermograph was built for the first time in 1937 by *A.F. Spilhaus*. Clear understanding of absorption of sound in the sea was achieved. And accurate values of absorption coefficients were determined at the ultrasonic frequencies.

By the start of the World War II, a large quantity of sonar sets was produced in the United States, and a large number of American ships were installed with both underwater listening and echo ranging. QC equipment was the standard echo ranging sonar set for surface ships. The operator searched with it by turning a handwheel and listening for echoes with headphones or loudspeaker. They noted the echoes range by the flash of a rotating light or by the range recorder. Submarines was installed with JP listening sets, which consisted of a rotatable horizontal line hydrophone, an amplifier, a selectable bandpass filter, and a pair of headphones. The period of World War II had a huge importance to underwater sound. In United Stated, a large group of scientists arranged by the National Defense Research Committee began researching on all phases of the subject. Most of nowadays concepts and applications had their origin from that period. Developments of World War II period was such as acoustic homing torpedo, the modern acoustic mine, and scanning sonar sets. Understanding of the factors in the sonar equation that affects the sonar performance was gained.

Years after World War II had some important developments of underwater sound, both for military and nonmilitary uses. On the military side, active sonars became larger, and more powerful. They could operate at lower frequencies than in World War II. Also passive sonars started to operate at lower frequencies so they could take the advantage of the tonal or line components in the low-frequencies submarine noise spectrum. The development of complex signal processing, in both time and space, made it poosible to enable much more information, which can be used for whatever function the sonar is called up to perform. The research of sound propagation in the sea has led to the exploitation of propagation paths.

Examples of developments of underwater sound for nonmilitary purposes after the World War II are:

1. Depth sounding
    - Conventional depth sounders
    - Subbottom profilers

    - Side-scan sonars
2. Acoustic speedometers
3. Fish finding
4. Fisheries aids
5. Divers' aids
6. Position marking
    - Beacons
    - Transponders
7. Communication and telemetry
8. Control
9. Miscellaneous uses

Examples of developmets of underwater sound for military purposes after World War II are:

1. Pressure mine
2. Acoustic mines
3. Minesweeping
4. Passive detection
5. Homing torpedoes
6. The underwater telephone
7. Neutrally buoyant flexible towed-line array

3.2 Basic physics of sonar

Sound is pressure perturbations that travels as a wave. Sound is also referred to as compressional waves, longitudal waves, and mechanical waves. A sound wave can be characterized by the following parameters:

- Wave period, $T[s]$
- Frequency, $f = \frac{1}{T}[Hz]$
- Sound speed, $c[m/s]$
- Wavelength, $\lambda = \frac{c}{f}[m]$

3.2.1 The Decibel unit

The desibel has been long used for reckoning quantities. Decibel makes it possible to handle large change in variables, and allows to multiply quantites by simply adding the decibel value together. Since acoustic signal strength varies in several orders of magnitude over a typical distance travelled, the decibel unit is used for sonar purposes. The notation of decibel is dB, and is defined as:

$$I_{dB} = 10log_{10}(I) \tag{3.1}$$

In Equation 3.1, the I_{dB} is intensity in dB and I is linear intensity. The decibel unit also makes it easier to see how much two quantites differ in dB. For example if I_1 and I_2 are two intensities, by taking dB of their ratio such as, $N_{dB} = 10log_{10}(I_1/I_2)$, you find that I_1 and I_2 differs by N dB.

3.2.2 Spherical- vs cylindrical spreading

Spherical- and cylindrical spreading are used to describe decrease of signal level as the sound wave propagates away from the source.

Spherical spreading

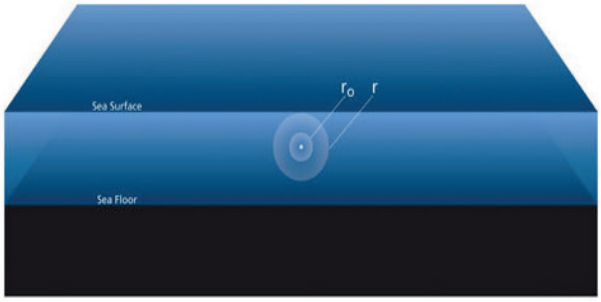

Figure 3.1: Spherical spreading, figure taken from [**?**]

Spherical spreading describes the decrease of signal level when the sound wave propagates uniformly in all directions, shown in Figure 3.1. The total power crossing any sphere around the source is given as, $P = 4\pi r^2 I$. And let I_0 be the intensity of the wave at range, r_0. If there is no absorption in the medium then the total power crossing each sphere is the same. From this I get, $P = 4\pi r_0^2 I_0 = 4\pi r^2 I$. If I solve this for I, I get:

$$I = I_0 \left(\frac{r_0^2}{r^2} \right) \tag{3.2}$$

The intensity decreases as the inverse square of the range for spherical spreading. If I say that $r_0 = 1m$, than I_0 is just the acoustic source level.

Transmission loss is the amount by which the intensity decreases to its level at the source and is expressed in dB:

$$\begin{aligned} TL_{dB} &= -10log_{10}(I/I_0) \\ &= 10log_{10}(r^2) \\ &= 20log_{10}(r)dB \end{aligned} \tag{3.3}$$

From this I can conclude that sound intensity I decreases with range R in inverse proportion to the surface of the sphere as $I \sim \frac{1}{R^2}$. This is for the one way spherical spread as illustrated in Figure 3.2. It is important to know that the relation between sound intensity I and signal amplitude A is $I = A^2$. Thus Equation 3.2 becomes:

$$\begin{aligned} A^2 &= A_0^2\left(\frac{r_0^2}{r^2}\right) \\ \Rightarrow \frac{A}{A_0} &= \frac{r_0}{r} \end{aligned} \tag{3.4}$$

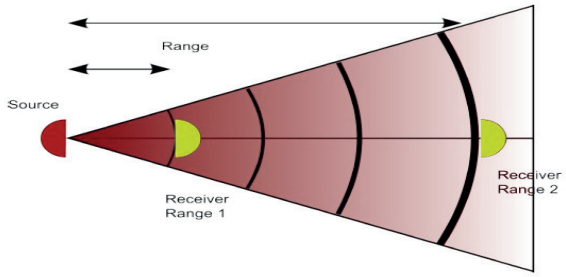

Figure 3.2: One way spreading loss, figure taken from *Hansen (2009)[?]*

For two way propagation, as illustrated in Figure 3.3, the wave propagates spherically to the reflector and the reflector spreads the signal in all directions and propagates spherically back to the source. The two way loss becomes, $I \sim \frac{1}{R^2}\frac{1}{R^2}$.

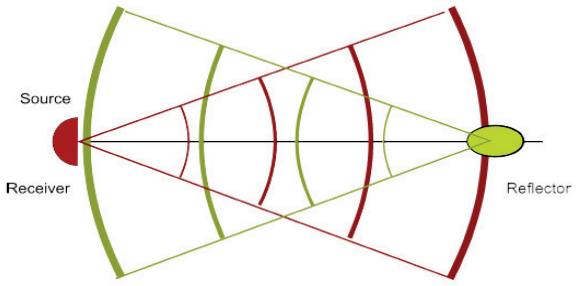

Figure 3.3: Two way spreading loss, figure taken from *Hansen (2009)[?]*

Cylindrical spreading

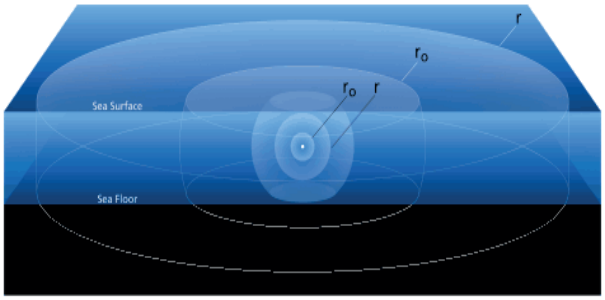

Figure 3.4: Cylindrical spreading, figure taken from [**?**]

Cylindrical spreading is just made out of the fact that sound cannot travel uniformly in all directions forever. At some point the wave will hit the sea surface or the sea floor. An approximation for spreading loss in that case is to assume that the wave propagates cylindrically away from the source with radius equal to range, r and height equal to depth, H, as shown in Figure 3.4. The total power crossing a cylinder around the source is given as, $P = 2\pi rHI$. As same as spherical spreading, the total power crossing each cylinder is equal, so I get: $P = 2\pi r_0 HI_0 = 2\pi rHI$. Solving for I gives:

$$I = I_0\left(\frac{r_0}{r}\right) \tag{3.5}$$

The intensity decreases as the inverse power of the range for cylindrical spreading. As same as spherical spreading, I say $r_0 = 1m$, and I_0 is the source level, than the transmission loss in dB becomes:

$$\begin{aligned} TL_{dB} &= 10log_{10}(I/I_0) \\ &= 10log_{10}(r)dB \end{aligned} \tag{3.6}$$

3.3 Underwater sound propagation

3.3.1 Absorption

Seawater is a dissipative medium through viscosity and chemical processes. Acoustic absorption in seawater is frequency dependent. Low frequencies reaches longer than high frequencies, *(Hansen, 2009) [**?**]*. The absorption coefficient is given in Equation 3.7, and is a function of temperature, salinity, depth (pressure) and pH value of the water along with frequency. The absorption coefficient formula given in *Fisher and Simmons (1977) [**?**]*, is as follows:

$$\alpha = \frac{A_1 P_1 f_1 f^2}{f_1^2 + f^2} + \frac{A_2 P_2 f_2 f^2}{f_2^2 + f^2} + A_3 P_3 f^2 \tag{3.7}$$

The parameter α is the absorption coefficient, and the first term in the equation is absorption caused by Boric Acid, the second term is absorption caused by magnesium sulfate, and the third term is absorption in pure water. Parameters P_1, P_2 and P_3 are effect of pressure. Frequency dependency is shown by f_1 and f_2, which are the relaxation frequencies of Boric Acid and magnesium sulfate. The frequency f is simply the sound wave frequency. Values of A_1, A_2 and A_3 depends on water properties, such as temperature, salinity and pH of water.

3.3.2 Refraction and sound velocity in sea water

Sound refraction occurs between two media or layers with different sound velocity. As shown in Figure 3.5, some of the sound hitting the surface of the other media is reflected and some is refracted.

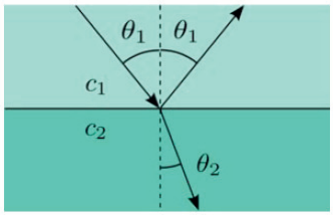

Figure 3.5: Snell's law, figure taken from *Hansen (2009)[?]*

How much bend the refracted sound wave will get depends on the incident angle and velocity at both layers:

$$\frac{\sin\theta_1}{c_1} = \frac{\sin\theta_2}{c_2} \tag{3.8}$$

The sound velocity in sea water depends on temperature T, salinty S and depth D, and is given in *Hansen (2009)[?]* as:

$$c = 1449.2 + 4.6T - 0.055T^2 + 0.00029T^3 + (1.34 - 0.010T)(S - 35) + 0.016D \tag{3.9}$$

Speed of sound in sea water is approximately between $1450 m/s$ and $1500 m/s$.

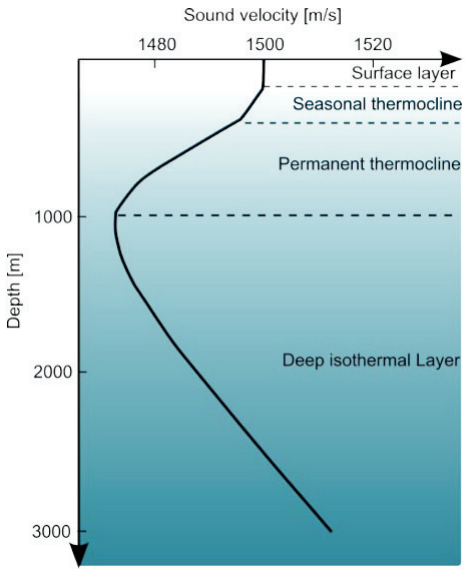

Figure 3.6: Sound velocity in the sea as function of depth, figure taken from *Hansen (2009)[?]*

As shown in Figure 3.6, the sea water sound velocity is divided into four different regions:

The surface layer	In this layer the sound velocity is exposed by daily and local changes of heating, cooling and wind actions. This layer may contain a mixed layer of isothermal water. Sound tends to be trapped or channeled in this mixed layer. The mixed layer disappears under sunny conditions, and is replaced by water where temperature decreases with depth.
The seasonal thermocline	Characterized with negative thermal or velocity gradient that varies with the season. It means that temperature and velocity decreases with depth
The permanent thermocline	Affected only slightly by seasonal changes. In this layer, occurs the major increase in temperature.
The deep isothermal layer	Has constant temperature about $3.89°C$. In this layer the sound velocity increases with depth because of the effect of pressure on sound velocity.

Table 3.1: Sound velocity profile in deep sea water.

In the area between the permanent thermocline and the deep isothermal layer, the sound travelling at great depths tends to bent by refraction.

3.3.3 Reflection

Figure 3.5 shows refraction and reflection. And as same as refraction, reflection occurs at the interface between to different media. At normal incidence, the reflection coefficient is given as:

$$V = \frac{Z - Z_0}{Z + Z_0} \tag{3.10}$$

The transmission coefficient is:

$$W = \frac{2Z_0}{Z + Z_0} = 1 - V \tag{3.11}$$

In Equation 3.10 and Equation 3.11, parameters Z and Z_0 are the characteristic impedances of the two media and are given by the sound velocity and density:

$$Z_0 = \rho c \tag{3.12}$$

Characteristic impedance for different materials is given in Table 3.2. From Equation 3.10, we can calculate the reflection coefficient between air and seawater. The result will be $V = -1$, which means that the sea surface is a "perfect" reflector.

Material	Impedance
Air	415
Seawater	1.54×10^6
Sand	5.5×10^6
Sandstone	7.7×10^6
Steel	47×10^6

Table 3.2: Characteristic impedance of different materials.

3.3.4 Scattering

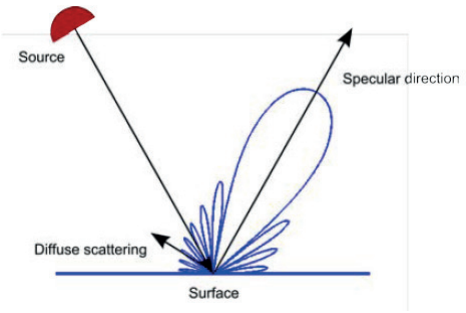

Figure 3.7: Scattering from a smooth surface, figure taken from *Hansen (2009)*[**?**]

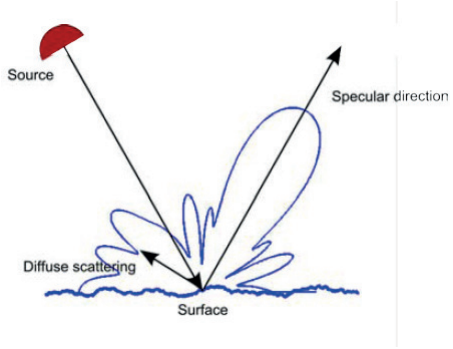

Figure 3.8: Scattering from a rough surface, figure taken from *Hansen (2009)[?]*

Scattering can be of two categories:

1. *Surface scattering* from the sea surface or the sea floor.
2. *Volume scattering* from ocean fluctuations, marine life or objects.

If the surface is smooth, as in Figure 3.7, then we will get specular reflection. And if the surface is rough as in Figure 3.8, then some part of the reradiated energy will be scattered diffusely in random directions. The more rough the surface is, the more energy will be scattered diffusely.

"A criterion for roughness or smoothness of a surface is given by the Rayleigh parameter, defined as $R = kH\sin\theta$, where k is the wave number $2\pi/\lambda$, H is the rms "wave height", and θ is the grazing angle. When $R \ll 1$, the surface is primarly a reflector and produces a coherent reflection at the specular angle equal to the incident angle. When $R \gg 1$, the surface acts as a scatterer, sending incoherent energy in all directions". *Urick (1983) [?].*

3.4 Sonar principles

We have two types of sonar systems, *passive sonar* and *active sonar*. *Passive sonar* is where a noise source is radiated by the target and received by the sonar. *Active sonar* is where the sonar transmits the signal, and the signal hitting the target reflects back, and is received by the sonar. In other words, passive sonar only receives the signal, and active sonar both transmits and receives the signal. When active sonar is used to measure distance from the transducer to the bottom, it is called "echo sounding". Active sonar is used for measuring distance between two transducers or a combination of hydrophones. Passive sonar are used for military settings and in science applications such as detecting fish in the ocean. Examples of Passive- and active sonar is shown in Figure 3.10 and Figure 3.9.

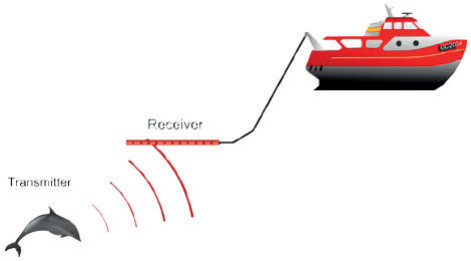

Figure 3.9: Passive sonar, figure taken from *Hansen (2009)*[**?**]

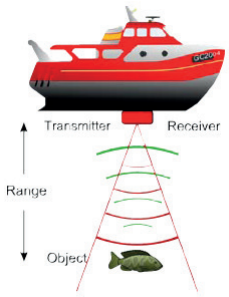

Figure 3.10: Active sonar, figure taken from *Hansen (2009)*[**?**]

3.4.1 Range estimation

Radial distance between sonar and reflector is defined as the range. Assuming that we are transmitting a short pulse with pulse duration, T_p. The receiver records the signal until the reflected echo is received and estimates the time delay, τ from the time series. The range to the target is then defined as:

$$R = \frac{c\tau}{2} \tag{3.13}$$

Where c is the sound velocity in the water.

If the purpose is to transmit two echoes, and in order to detect those two echoes, they has to be seperated by a minimum distance or range defined as the range resolution:

$$\delta R = \frac{cT_p}{2} \tag{3.14}$$

Shorter pulses gives better resolution, but shorter pulses have less energy in the pulse, which again gives shorter propagation range. Alternatively, we can phase code the pulse and resolution becomes:

$$\delta R = \frac{c}{2B} \tag{3.15}$$

Where B is the bandwidth of the acoustic signal, and relates to the pulse duration as, $B = \frac{1}{T_p}$ for gated Continuous wave (CW) signals.

3.4.2 Bearing estimation

By bearing estimation, it means estimating the direction of sonar pulses. It has two key elements involved:

1. The electro-acoustic transducer and its size.
2. The grouping of transducers and its size.

It is said that a sonar source (*e.g.* transducer, antenna or loudspeakers) is directive if the size of the source is large compared to the wavelength of the signal. The directivity pattern of a source, with diameter or size D, has a main lobe with a -3 dB *beamwidth* or *field of view* as:

$$\sin\beta \approx \frac{\lambda}{D} \tag{3.16}$$

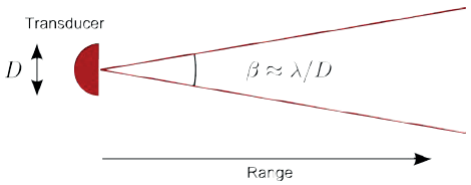

Figure 3.11: Main lobe pattern of a single transducer, figure taken from *Hansen (2009)*[**?**]

If we have a source with N equally spaced (spacing distance of d_s) elements with size D, then *beamwidth* or *field of view* becomes:

$$\sin\beta \approx \frac{\lambda}{ND + Nd_s} \tag{3.17}$$

It has to be marked that β is derieved in radians and not in degree. For small angles, it is mathematically proved that $\sin\beta \approx \beta$. From Equation 3.16 and Equation 3.17 it is clear that the beamwidth depends on frequency (since $\lambda = \frac{c}{f}$) and the total length of the array. So higher frequency or larger antenna array size gives narrower beam.

The bearing from a reflected signal is estimated from the time difference of arrival δt between two different receivers with distance L apart (illustrated in Figure 3.12):

$$\theta = \sin^{-1}\left(\frac{c\delta t}{L}\right) \tag{3.18}$$

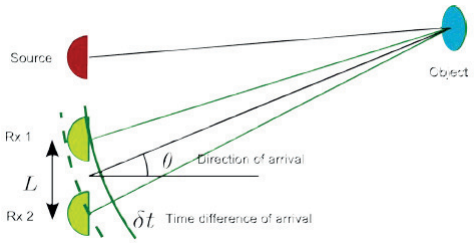

Figure 3.12: Direction of arrival, figure taken from *Hansen (2009)[?]*

3.4.3 Imaging sonar

Imaging in sonar is to estimate the reflectivity for all calculated ranges and in all directions. There are several methods to do so, such as delay and sum (backprojection) and wavenumber-domain beamformers. Imaging sonar is described in Figure 3.13.

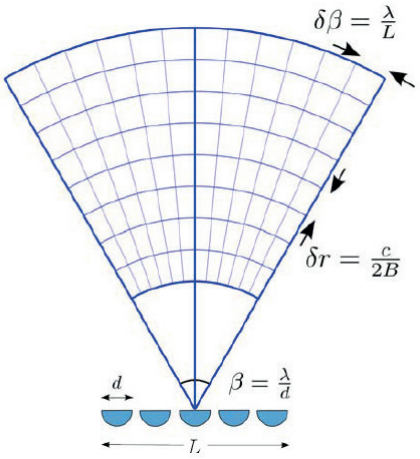

Figure 3.13: Imaging sonar, figure taken from *Hansen (2009)[?]*

As shown in Figure 3.13, the field of view is given by the angular width of each element as $\beta = \frac{\lambda}{d}$. The angular or azimuth resolution is given by the array length as $\delta\beta = \frac{\lambda}{L}$, and the range resolution is given by bandwidth of the system as $\delta r = \frac{c}{2B}$.

Chapter 4

The sonar equation

The sonar equation was first formulated during the World War II for calculation of maximum range of sonar equipments. The sonar equation shown in this thesis are taken from *Urick (1983)*. In *Urick (1983)* it states that, "the main phenomena and effects peculiar to underwater sound produce a variety of quantitative effects on the design and operation of sonar equipments". *Sonar parameters* are units of these effect, and are related to the *sonar equations*. The basic foundation of sonar equation is the quality between desired (signal) and undesired (background) parts of the recieved signal. A portion of the total acoustic field at the receiver is said to be the signal, and rest is said to be the background. For sonar to successfully detect a signal, the signal level has to be larger than the background level.

There are two types of background levels that masks the signal, *noise background* and *reverberation background*. Noise background or noise level is isotropic sound generated from wind, waves etc. Reverberation background or reverberation level is the slowly decaying portion of the backscattered sound from one's own acoustic input. Figure 4.1 shows the echo-, noise- and reverberation level as a function of range. It is shown that the echo level and reverberation level falls with increasing range, but the noise level is constant for all ranges. The echo level falls off much before the reverberation level, and they intersect each other at range R_r. The echo level intersect the noise level after range R_r, it is not marked in the figure but it is the point where echo level is equal to the noise level. If the reverberation is high, the range is said to be reverberation limited. And if by any reason the noise level rises to the level shown by the dashed lines, the echoes will rather die away into noise background rather than reverberation background. The noise limited range R_n will then be smaller than reverbeartion limited range R_r and the range will become noise limited.

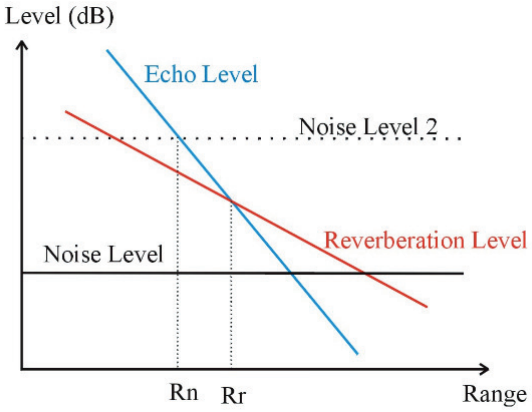

Figure 4.1: Echo, noise and reverberation as function of range, figure taken from [**?**].

4.1 Sonar parameters

The sonar parameters are the effects from the medium, target and the equipment.

Parameters determined by the *medium* are:

- Tansmission loss: **TL**
- Reverberation level: **RL**
- Ambient-Noise level: **NL**

Parameters determined by the *target* are:

- Target strength: **TS**
- Target source level: **SL**

Paramaters determined by the *equipment* are:

- Projector source level: **SL**
- Self-Noise level: **NL**
- Receiving directivity index: **DI**
- Detection threshold: **DT**

A source produces a source level SL, which is the acoustic intensity of the signal 1 meter away from the source. As the signal propagates towards the target the intensity is reduced by the range, and the loss of intensity is called transmission loss TL. TS is the target strength of the reflected signal 1 meter from the target. On the way back the signal again is reduced by the transmission loss TL, and thus the echo level at the transducer becomes $SL-2TL+TS$. On the background side, the background level is simply NL, and is reduced by the directivity index DI. So the echo-to-noise ratio at the transducer terminals becomes:

$$SL-2TL+TS-(NL-DI) \tag{4.1}$$

4.2 Three types of sonar equations

There are three types of sonar equations:

- The active sonar equation for noise background.
- The active sonar equation for reverberation background
- The passive sonar equation

4.2.1 The active noise background sonar equation

This is the most commonly used sonar equation. And the signal-to-noise ratio in Equation 4.1 defines whether the target is absent or present. If the signal-to.noise ratio is less than the detection threshold DT, then the target is said to be absent. But if the signal-to-noise ratio equals the detection threshold, the target is said to be present. The sonar equation becomes:

$$\begin{aligned} SL-2TL+TS-(NL-DI) &= DT \\ SL-2TL+TS &= NL-DI+DT \end{aligned} \tag{4.2}$$

4.2.2 The active reverberation-background sonar equation

In this case we replace a noise background with reverberation background. Thus, the parameter DI is not needed, and the term $NL-DI$ is replaced by reverberation level RL. The active sonar equation then becomes:

$$Sl-2TL+TS=RL+DT \tag{4.3}$$

Here it has to be marked that DT value in reverberation is different from the noise background DT.

4.2.3 The passive sonar equation

In this case, the target itself creates the signal , and the SL now refers to the level of the radiated noise of the target 1 meter away. The TS becomes irreleveant, and the transmission loss is now one-way not two-way loss. The passive sonar equation becomes:

$$SL - TL = NL - DI + DT \tag{4.4}$$

Part III

The Experiment

Chapter 5

Background for the experiment

The purpose of the experiments or the concept of this thesis is to find whether it is possible to detect a sound signal in water which is transmitted from a circular transducer with an incident angle of 180° to the receiver. And to study how sound propagates in this situation. Does it travel along the surface of the transducer or does it bend in water to reach the receiver? Can this be compared to human listening?

All experiments was done in the DSB lab at ifi on the 4th floor. All equipments used in the experiments are described in this chapter as well as all assumptions that has been made. I will also go through a quick section of how simulation was done on Matlab.

5.1 Equipments

Equipments or tools used in the experiments were:

- Tank in DSB lab
- Transducer as a transmitter
- The tube which protects the electronics in the transducer from water
- Hydrophone as a receiver
- Connector to connect transducer to the generator
- Oscilloscope
- Preamplifier
- Signal generator
- JBL sound amplifier
- Programming language, Matlab

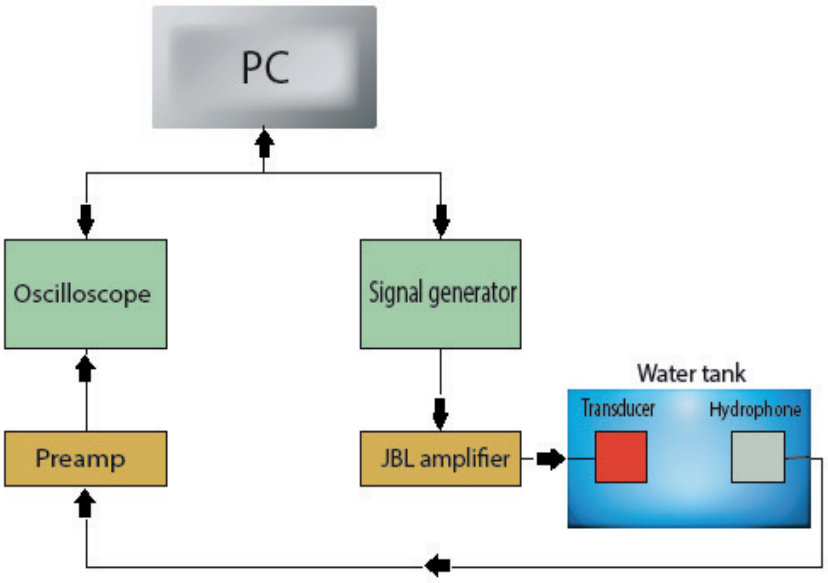

Figure 5.1: The system diagram

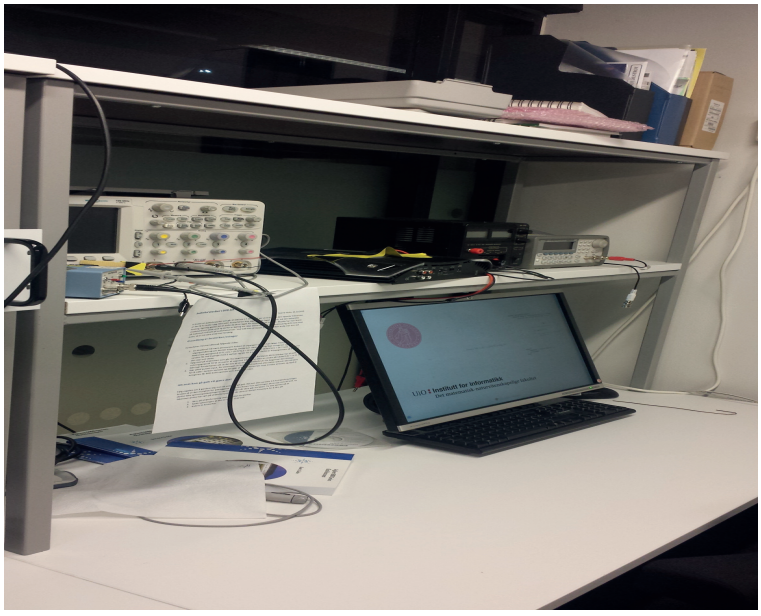

Figure 5.2: The connection betweem computer and instruments.

In Figure 5.1, I have illustrated how the system is connected together. Both the signal generator and the oscilloscope are connected with the computer, and controlled by a matlab program which I will come back to later in this chapter. The signal generator sends a signal to the amplifier, which sends it to the transducer. The signal from the transducer is then

received by the hydrophone, which is connected to a preamplifier, and then to the oscilloscope. First of all, to connect the transducer we had to buy a pin connector, and then make a electronic circuit to connect the transducer with the amplifier. The electronic circuit is shown in Figure 5.3, and is connected with pin connector in the bottom.

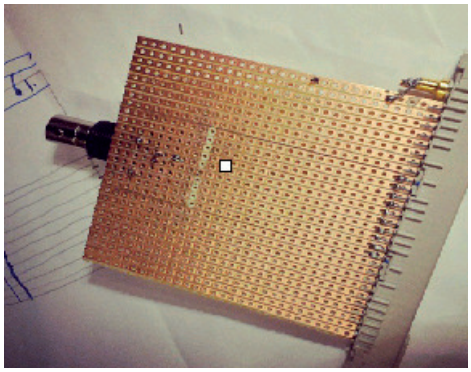

Figure 5.3: Electric circuit with a pin connector

5.1.1 The Tank

Tank which was used is mounted on the DSB lab at ifi on the 4th floor. It is a small tank with dimensions, along the sink wall, $x = 149.7cm$ and the long side, $y = 187.4cm$. The picture of the tank is shown in Figure 5.4 and in Figure 5.5 you can see an illustration of the tank. The coloured boxes on the top is obstacles such as pipes, light bulbs and other obstacles.

Figure 5.4: The water tank in the lab

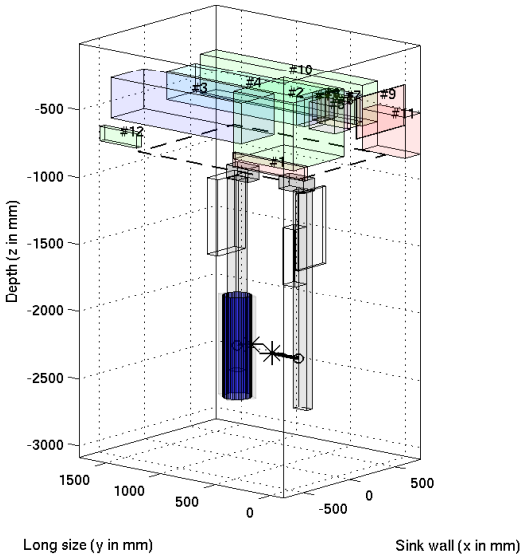

Figure 5.5: The tank illustration in matlab made by professor Svein Bøe

There are mounted two probes in the tank, as you can see in Figure 5.5. On one of them we have installed the transducer, and on the other we have installed the hydrophone. How they are used is described later. The tank is filled up with water at a height of 120 cm, and to avoid as much reflections as possible, the source is positioned in the middle of the tank with a depth of 60 cm. The receiver is placed 21.4 cm away from the source, and has to be placed within the beamwidth of the source (which is shown in the next section).

5.1.2 Transducer

Figure 5.6: The transducer, Simrad SH90 mounted on the bottom of the tube.

Most challenging part of my thesis was to find the correct transducer. I am using a circular transducer named *Simrad SH90* which is borrowed from *Kongsberg Maritime AS*. As you can see in Figure 5.6 the transducer is the red instrument mounted on the bottom of the tube. Further technical information is given in the Kongsberg Maritimes' webpage, http://www.simrad.com/sh90.

The transducer consists of 480 channels or elements which are uniformly distributed around the transducer. Simrad SH90 consists of 8 sectors, which again consists of 6 stripes each. Assuming that all elements are equally spaced and distributed then each stripe consists of $\frac{\frac{480}{8}}{6} = 10$ elements/channels. In this thesis I have assumed that this 10 sensors are equally distributed vertically at the transducer on each stripe. It has to be noted that in the experiments I have only used one strip, which is stripe nr. 3 on sector nr. 2. Further study of the Simrad SH90, gives us that every stripe is spaced to each other by an angle of $\frac{360°}{48 pins} = 7.5°$. Stripe nr. 1 in sector 2 is located at $3.5°$, and stripe nr. 3 in sector 2 is located at $18.5°$ and stripe nr. N is located at $(3.5° + (7.5°(N-1)))°$. How elements are distributed in the horizontal and vertical plane is illustrated in Figure 5.7.

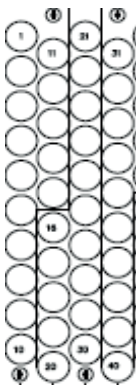

Figure 5.7: Elements of Simrad SH90

Dimensions of the transducer

The Simrad SH90 transducer has a diameter of $d = 12cm$, which gives the radius, $r = 6cm$. This gives the circumference (perimeter) of the transducer as, $O = 2\pi r = 2\pi \times 6cm = 37.7cm$. The height of the transducer is $21cm$, and the elements are located at the vertical extent of $11cm$ and the rest is covered by other things such as, electronic parts, wires etc. It is markable to note that in this thesis I have assumed that each element has same depth, height and width equal to $1cm$. I am assuming this because there are no given information about the dimension of any element/channel in the

specifications. But we will see later in this thesis that my assumption of size is almost correct.

Vertical beamwidth

Since I'm only using 10 elements, which are equally spaced and distributed in the vertical direction, and as mentioned above, the range where these elements are located is $L = 11cm$. From Equation 3.17, we know that, $L = ND + Nd_s$ where N = 10 in this case. Since $D = 1cm$, we get that the space between elements are $d_s = 0.1cm$. This is shown in Figure 5.8.

It is later shown that the wavelength, $\lambda = 1.488cm$, thus from Equation 3.16 (for small angles) the vertical beamwidth becomes:

$$\beta_{rad} = \frac{\lambda}{L} = \frac{1.488cm}{11cm} = 0.135rad \tag{5.1}$$

In degrees:

$$\beta_{deg} = \frac{180° \times 0.135rad}{\pi} = 7.73° \tag{5.2}$$

The beamwidth from the transducer is illustrated below:

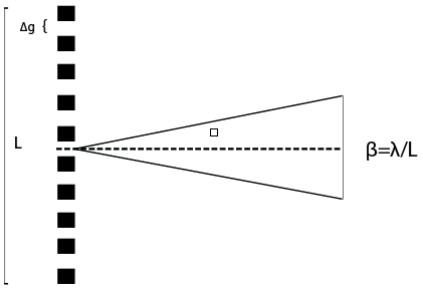

Figure 5.8: Vertical beamwidth with ten sensors arranged vertically and equally spaced

Horizontal beamwidth

In the horizontal plane, the beamwidth is dependent only on one single element. This means that the beamwidth is supposed to be larger since the sensor size becomes smaller. An approximation of how it will look like is illustrated in Figure 5.9.

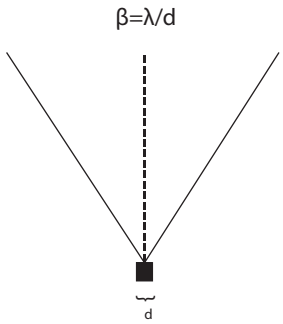

Figure 5.9: Horizontal beamwidth with sensor size d

But this is not the case here. The size of the sensor element is $d = 1cm$, which gives $\lambda > d$. The $\sin\beta > 1$, which is an invlaid value for sinus. The beam is larger than $90°$, and covers the whole area around the transducer. This is further studied in experiment III on chapter 8.

Protection of Simrad SH90

One thing we were recommended by our professors was to protect the transducer from water when we don't do any experiments. It was challenging to find out how we could clear water around the transducer when we finished the experiments everytime. We could not lift the transducer up because of the limits of the probe and the obstacles on the ceiling. So what we did, was to buy a fender (which is used on boats), with dimensions accordingly for the transducer, the tube and the amount of water in the tank. By cutting the top, we had an opening that fitted the dimesions of the transducer. The main idea was to cover the transducer with the fender while the transducer was in the water, and by using the Hevert principle we could take out the water inside the fender. Figure 5.10 shows how it looked like when the transducer was covered by the fender:

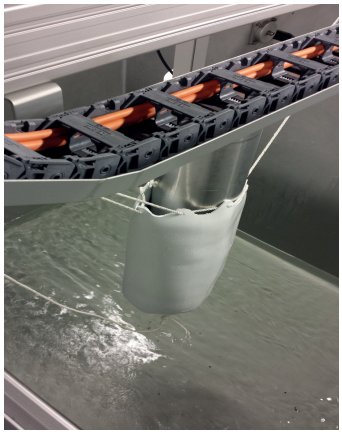

Figure 5.10: The transducer covered by the fender

5.1.3 The tube

The tube was also borrowed by the *Kongsberg Maritime AS*, and was used to protect the electronics of Simrad SH90 from the water. The tube was made water proof and the dimensions of the tube are, height equals $53.5cm$ and the diameter is $22cm$. A picture of the tube is shown in Figure 5.6.

5.1.4 The hydrophone

The hydrophone used was the Teledyne Reson TC4034. The datasheet of the TC4034 can be downloaded from Teledynes' webpage, http://www.teledyne-reson.com/products/hydrophones/tc-4034/. In the thesis we have assumed that the elements are located in front at the hydrophone since there are no information given to us about the location of the elements. A picture of the hydrophone mounted on the probe is shown in Figure 5.11.

Figure 5.11: The hydrophone, Teledyne Reson TC4034

As same as the transducer, the hydrophone has to be water free when not used. That was easy in this case since the probe it was mounted on could be positioned all the way up to the ceiling so the hydrophone could be placed outside the water.

5.2 Simulation process in the tank

The position system was programmed by professor Svein Bøe in Matlab. We used the latest version 13.49. The system was programmed in the manner that we could position the hydrophone by giving its position on the program. Even rotating was done in the matlab program. But for the transducer we could only rotate by using matlab, for positioning we had

to do it physically, and measure its position. This was a bit challenging, and because of that we had to do the experiments several times. We did some changes in the code where we thought it needed changes, such as for capturing the data from the oscilloscope.

5.3 Input signal

We are generating a sinus pulse through signal generator with cycles, $N = 3$. The signal frequency is $f = 100kHz$ with a peak to peak value $V_{pk-pk} = 500mV$. As shown later in the thesis, the sound velocity in water is $c = 1488m/s$. The wavelength of the signal in water is given as $\lambda = \frac{c}{f} = \frac{1488m/s}{100kHz} = 1.488cm$. I am using a burst period of $1s$. As mentioned the sinus signal is amplified by an audio amplifier, which gave us the signal in Figure 5.12. From this figure we can see the amplitude of the signal input is $V_{pk-pk} = 17.2V$.

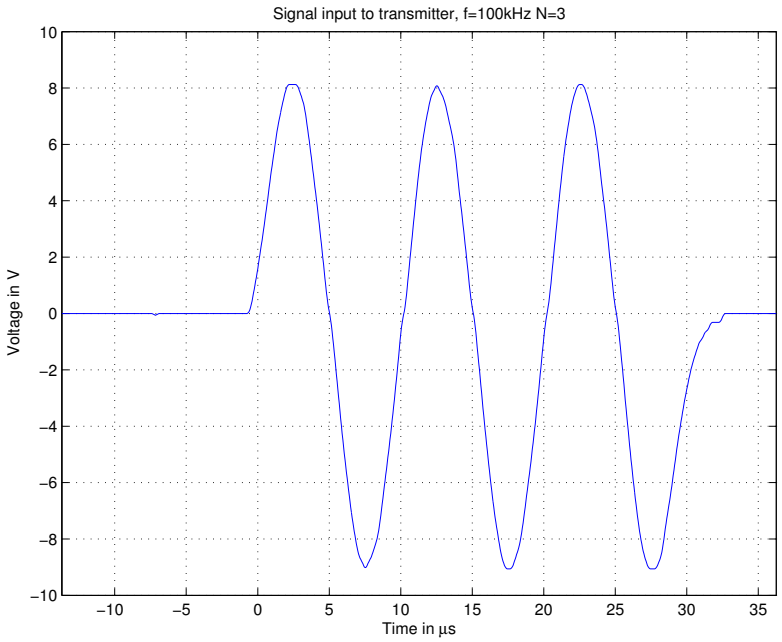

Figure 5.12: Input signal

Chapter 6

Geometry

In this chapter I am going to show some geometrical cases and calculations (such as distance caluclation, tangent caluclation, Sound path cases etc.).

6.1 Distances from source to receiver

In this section I am going to calculate the distances from the source to the receiver while rotating the transducer. The hydrophone is placed at a distance $x_0 = 21.4cm$ from the transducer source. And as said before the radius of the transducer is, $r = 6cm$. The parameters and the geometry between the transducer and the hydrophone is illustrated in Figure 6.1.

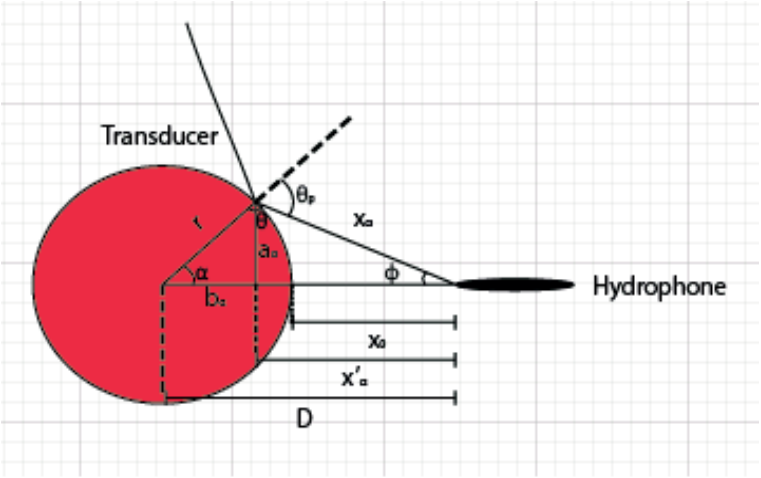

Figure 6.1: Geometry of the distance between transmitter and receiver

The parameters in the figure above are:

- The distance $x_0 = 21.4cm$
- The radius of the transducer, $r = 6cm$

- The distance $D = r + x_0 = 27.4cm$
- Angle α is the rotational angle of the transducer
- Angle $\theta = 180° - \theta_p = 180° - \alpha - \phi$
- Angle $\theta_p\,(= \alpha + \phi)$ is the beam angle of the transmitted signal
- The distance $a_\alpha = r \times \sin\alpha$
- The distance $b_\alpha = r \times \cos\alpha$
- The distance $x'_\alpha = D - b_\alpha$
- The distance $x_\alpha = \sqrt{a_\alpha^2 + x_\alpha'^2}$

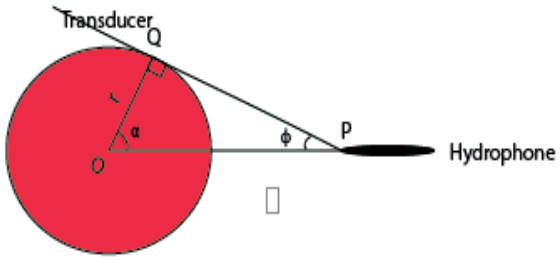

Figure 6.2: Tangent on the transducer to hydrophone.

First of all, I have to find the tangent of the signal transmitting from the source. That is at which rotating angle α, the signal is not travelling directly to the receiver. It means that the receiver is unseen by the source.

The Figure 6.2 shows the geometry of finding the tangent.

In this case $\theta = \theta_p = 90°$, and $\alpha = \alpha_{tangent}$ can be found by:

$$x_{\alpha_{tangent}} = \sqrt{D^2 - r^2} = 26.7cm$$

$$\sin\phi = \frac{r}{D} = 0.22 \rightarrow \phi = 12.64°$$

$$\Downarrow$$

$$\alpha_{tangent} = \theta_p - \phi = 77.36^\circ \tag{6.1}$$

Now that we know the angle of tangent, I can calculate by some trigonometry the distances from the source to the receiver by rotating the transducer from $\alpha = 0^\circ$ to $\alpha_{tangent}$. It is not important to derive the distance for every angle, and therefore I have chosen some angles given in Table 8.1.

α	$a_\alpha(cm)$	$b_\alpha(cm)$	$b'_\alpha(cm)$	$x'_\alpha(cm)$	$x_\alpha(cm)$
0°	0	6	0	21.4	21.4
15°	1.55	5.79	0.21	21.61	21.67
30°	3	5.2	0.8	22.2	22.4
45°	4.24	4.24	1.76	23.16	23.54
60°	5.2	3	3	24.4	24.95
75°	5.8	1.55	4.45	25.85	26.49

Table 6.1: Parameters of Figure 6.1

The other important geometrical problem is what is the rotational angle α, when the hydrophone is at the -3dB point of the beamwidth or mainlobe. This problem is illustrated in Figure 6.3:

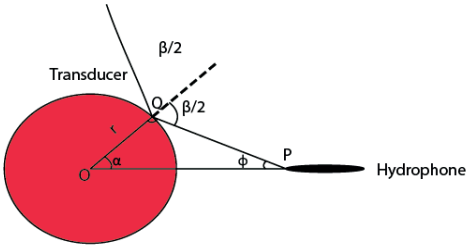

Figure 6.3: Beamwidth of the transducer

Here, $\theta_p = \frac{\beta}{2}$. I will come back to this problem later in chapter 8.

6.2 Sound propagation path

In this section I want to illustrate how sound can travel in water with signal transmitted when the rotational angle $|\alpha| \leq \alpha_{tangent}$ or with signal transmitted when rotational angle $|\alpha| > \alpha_{tangent}$. I will give some cases, which is only assumptions, and try to give explainations from graphs and the data I have received from the experiments. Some of those cases are there to show that they are incorrect compared to the data measured.

6.2.1 Sound path for angles, $\alpha \in [-\alpha_{tangent}, \alpha_{tangent}]$

In this interval sound travels either direct to the receiver or it travels along the surface of the transducer for a while and then travels direct to the receiver. In case I, as illustrated in Figure 6.4, the sound wave travels direct

to the receiver. And in case II, as illustrated in Figure 6.5, the sound wave travels along the surface of the transducer, until it reaches the 0° mark and then travels direct towards receiver.

Case I

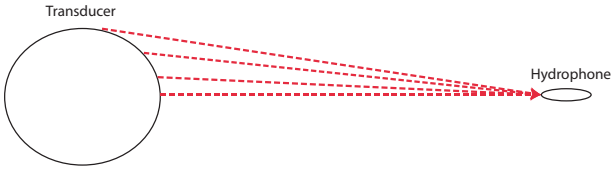

Figure 6.4: Case I: Sound wave travels direct to the receiver.

Case II

Figure 6.5: Case II: Sound wave travels first along the surface of the transducer, and then direct to the receiver.

6.2.2 Sound path for angles, $\alpha \in [\alpha_{tangent}, (360° - \alpha_{tangent})]$

In this interval I want to study two cases. In case III, as illustrated in Figure 6.6, the sound wave travels along the surface of the transducer until it reaches the $\alpha_{tangent}$, and then travels direct to the receiver. In case IV, as illustrated in Figure 6.7, the sound wave travels in the same way as in case III, but not on the surface of the transducer, but in water and bends in the same way as the surface of the transducer.

Case III

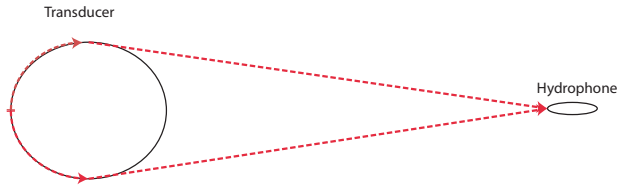

Figure 6.6: Case III: Sound wave travels on the surface of the transducer until it has a clear path to the receiver, and the direct to the receiver.

Case IV

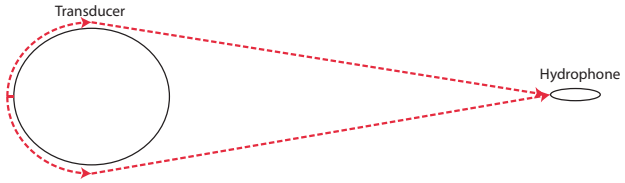

Figure 6.7: Cae IV: Sound wave travels the same path as case III, but in water.

Chapter 7

Pre-Experiments

7.1 Experiment I - Finding the beam direction

Before doing the experiment we have to find where the signal is strongest, and in which way the transducer transmits the signal. This experiment is done by rotating the transducer and by moving the receiver in different positions in height. I have picked som rotational angles for the transducer and some positions for hydrophone in matlab.

Angles picked for transducer is as follows:

$\alpha = [-35°, -28°, -21°, -14°, -7°, 0°, 7°, 14°, 21°, 28°, 35°]$

Figure 7.1 shows the signals in different angles and for each angle at different height positions. Figure 7.1 is just showing how the signal look like in different angles and height positions.

Figure 7.2 shows the amplitude value when moving the receiver in different height positions. The different graphs shows the different angles for transducer.

Figure 7.3 shows the intensity of the amplitude, which is given as, $I = A^2$. And Figure 7.4 shows a 3D plot of Figure 7.3.

By inspection of Figure 7.2, 7.3 and 7.4, the signal is absolutely strongest in 0° and when the receiver is placed at the same height as the middle of the transducer. Here -960 mm is equal to 60 cm from tank floor. The height parameter is for receiver probes head position given in the tank program.

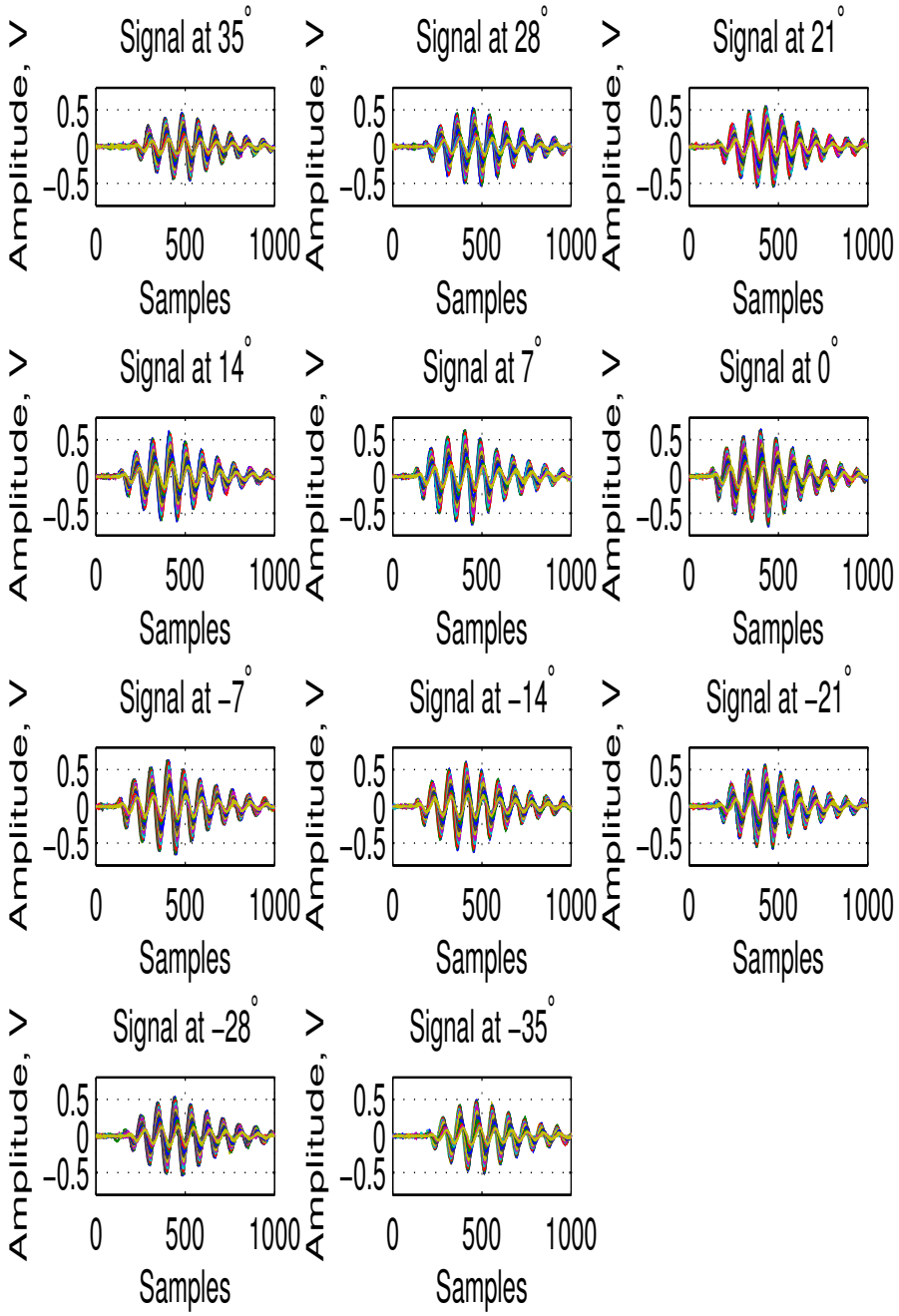

Figure 7.1: Signal in different angles and different heights

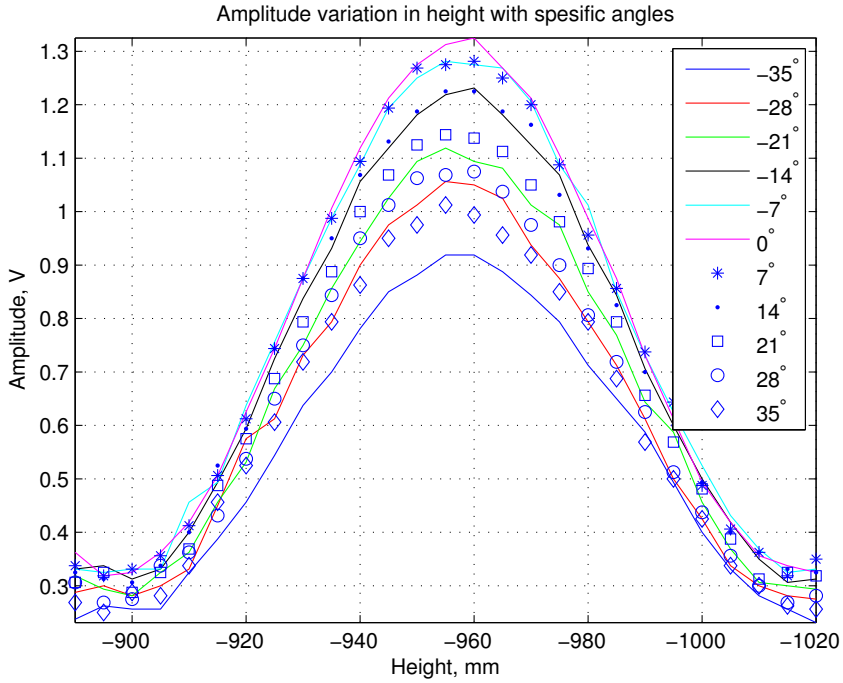

Figure 7.2: Inspection of maximum signal value I

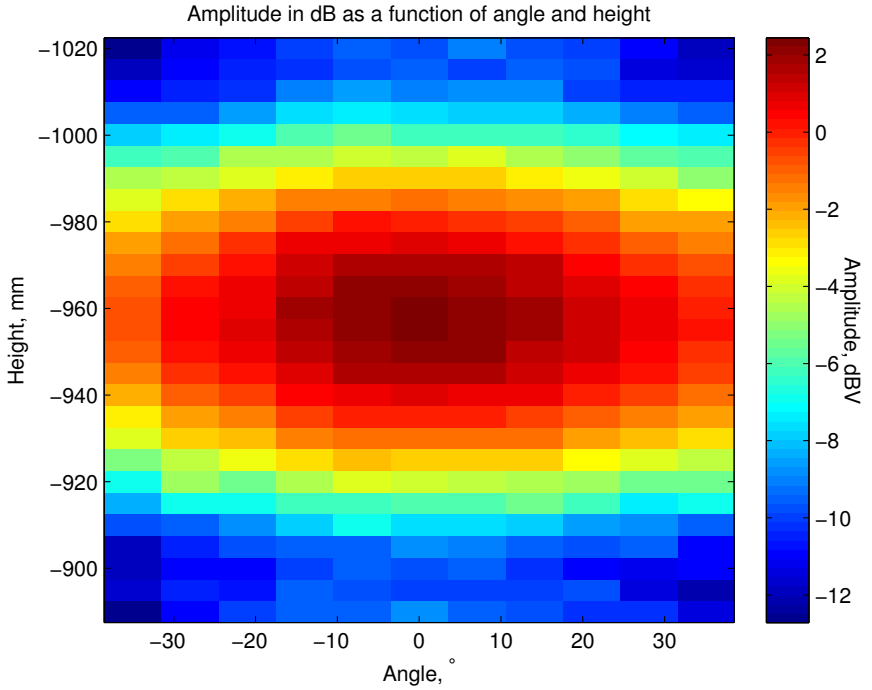

Figure 7.3: Inspection of maximum signal value II

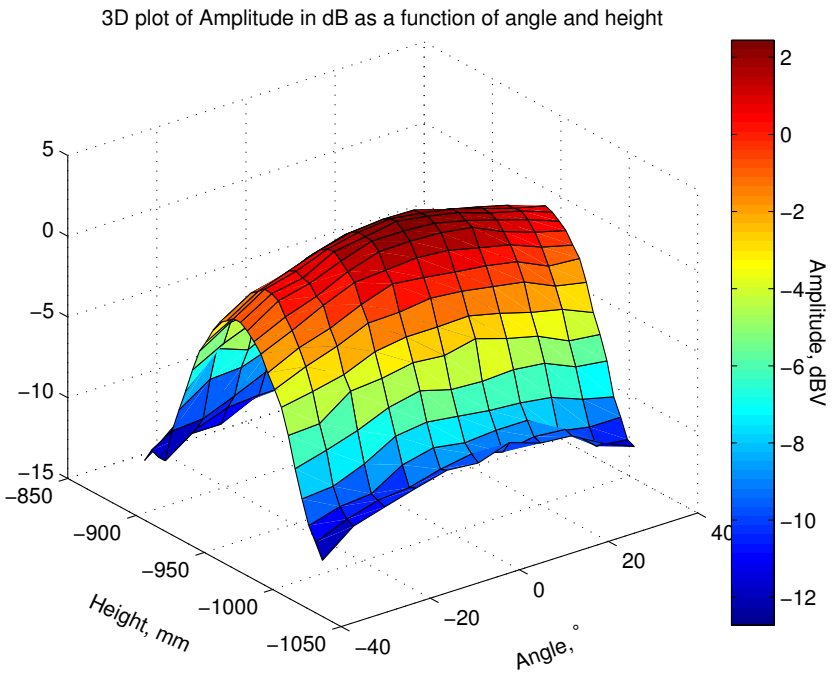

Figure 7.4: 3D plot of Figure 7.3

The amplitude should be symmetrical around 0°, since the distance is equal on both sides. But as shown in Figure 7.5, the amplitude is not symmetrically. Reason behind that can be that I didn't place the receiver in front of the transducer, or as I assumed the rotational angle 62° in matlab program of the tank may not equal to 0° of the transducer. To get the precice measurements, I could have rotated the transducer by smaller intervals, and where I would get the maximum value of the amplitude would be my 0°.

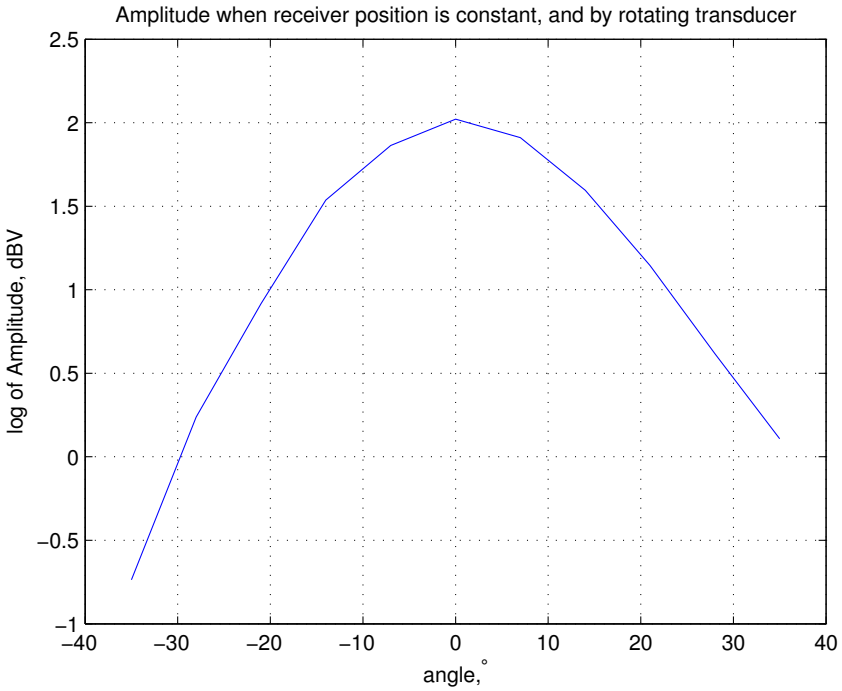

Figure 7.5: Amplitude plot as a function of angle

It has to be noticed that after doing the experiment we knew that we should have picked more values for the rotational angle. We can see from Figure 7.5, that the amplitude does'nt fall with -3dB which is the point for the mainlobe. In this experiment the distance between source and receiver is unknown, and therefore it is not possible to say how many angles we should take for.

7.2 Experiment II - Finding sound velocity

Sound velocity in water is approximately $1500 m/s$. To get an exact value of the sound velocity in the water tank I had to do some measurements with the transducer sending signals direct to the hydrophone. It means the angle of incidence, $\theta = 0°$. There are two methods for finding the sound velocity,

one is by measuring the temperature of the water and using Equation 3.9. Since we have a small water tank, we don't have to consider for depth, and since the experiments are done in pure water, the parameter of salinity is negligible. Equation 3.9 becomes:

$$c(T) = 1402.3 + 4.95T - 0.055T^2 + 0.00029T^3 \tag{7.1}$$

After filling the tank I placed a thermometer in the water and after some days I could read that the temperature was constant at $T = 19°C$. By using Equation 7.1 we find that the sound velocity in water is:

$$c(19°C) = 1402.3 + 4.95 \times 19°C - 0.0055 \times (19°C)^2 + 0.00029 \times (19°C)^3 = 1478.5 m/s \tag{7.2}$$

The other method is by measuring time received in two different positions for the hydrophone. First I placed the hydrophone at a distance, $x_1 = 21.4cm$ from the transducer and received the signal as shown in Figure 7.6. Signal was received at a time, $t_1 = 147\mu s$.

Secondly I moved the hydrophone at a distance, $x_2 = 41.4cm$ from the transducer and received the signal as shown in Figure 7.7. Signal was received at a time, $t_2 = 281.4\mu s$.

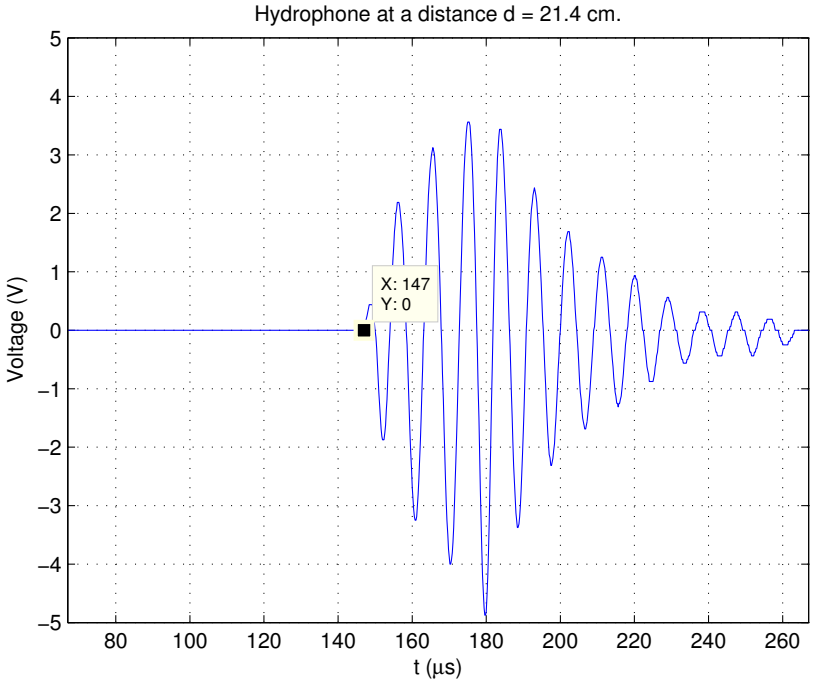

Figure 7.6: Signal captured at a distance of 21.4 cm

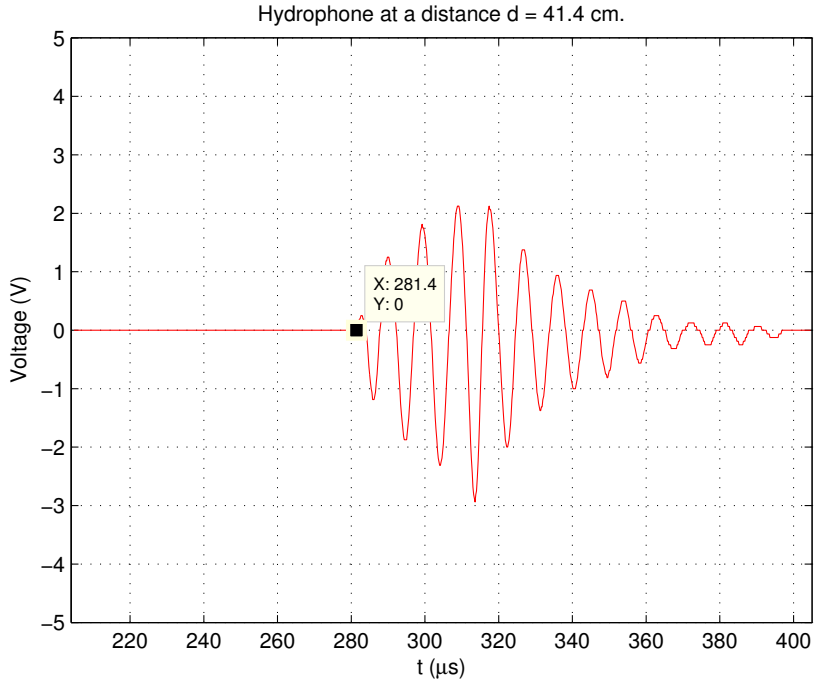

Figure 7.7: Signal captured at a distance of 41.4 cm

The sound velocity can be found by:

$$\begin{aligned}\Delta x &= x_2 - x_1 = 41.4cm - 21.4cm = 20cm \\ \Delta t &= t_2 - t_1 = 281.4\mu s - 147\mu s = 134.4\mu s \\ c &= \frac{\Delta x}{\Delta t} = \frac{20cm}{134.4\mu s} = 1488.1m/s \end{aligned} \tag{7.3}$$

We can see that the sound velocity for this two methods differs by a factor of $10m/s$. That's not bad, and the reasons for the difference could either be geometrically (Transducer and hydrophone not placed correct) or that the temperature measured differed with some value. The velocity I will use further in the thesis is $c = 1488m/s$.

Chapter 8

Main experiments

In this chapter I will show the main experiments of this thesis. Experiment III (where I rotate my transducer from $-90°$ to $90°$) is actually done to find the beamwidth of the transducer. By plotting the amplitude in dB I can find where the amplitude drops by $-3dB$ and then calculate the effective element size d_{eff}. Experiment III is also done to find the instrumental delay in all instruments, and to prove and disprove some of my geometrical calculations and cases in Chapter 6. In experiment IV (where I rotate my transducer from $85°$ to $275°$) I will show whether it is possible or not to capture the signal when the transducer is rotated $180°$. As well as finding the sound velocity for the diffracted wave and to prove and disprove some of the geometrical cases. I will also compensate amplitudes from both experiments by studying the difference.

8.1 Experiment III - Front experiment

This experiment was done by rotating the transducer from $-90°$ to $90°$ with an interval of $1°$. At first, the transducer was rotated by manually changing the parameters in Matlab. This took too much time, thus we made a program in matlab that rotated the transducer automatically. The program first captured the data from the oscilloscope, plotted it in the matlab and then rotated the transducer with an angle of $1°$. It was quite challenging since the signal sometimes got delayed because of the mechanism.

The program plotted every data in the matlab in one single figure. In the end we got 181 signals, which is shown in Figure 8.1. Every data/signal has 1000 samples, and is plotted as the received voltage on the hydrophone. The samples are converted into time with some simple processing, where the parameters from the oscilloscope is taken in consideration.

Figure 8.2 shows the signal in dB at every angle as function of time. From the figure it is confirmed that the signal at $0°$ reaches the receiver earlier than the other signals. As the positive angle increases, the signal gets more and more delayed. And as the negative angle decreases, the signal gets more and more delayed. We can also see that the signal intensity decreases by in-

creasing or decreasing the angle from 0°. It has two reasons, the first one is that the range increases as we decrease or increase the angle from 0°. The other one has something to do with the transducers directivity, which I don't have so much information about.

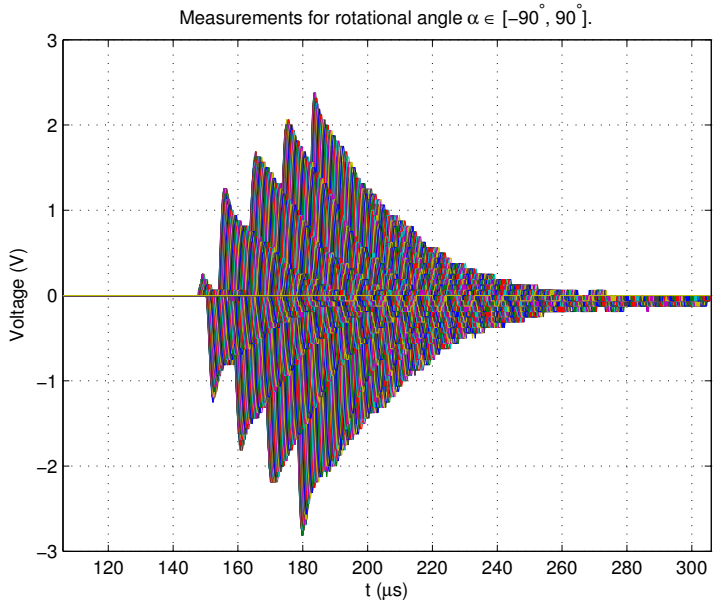

Figure 8.1: Signal captured by the oscilloscope

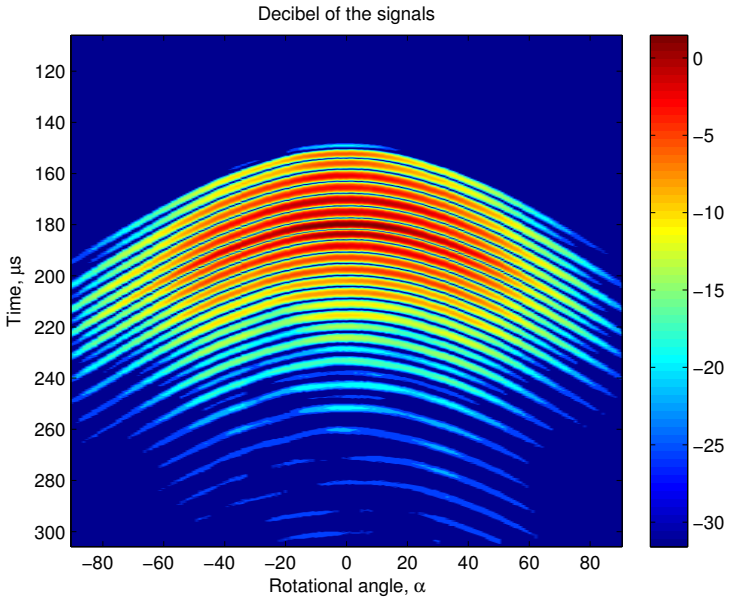

Figure 8.2: Signal in dB

8.1.1 Amplitude inspection and beamwidth calculation

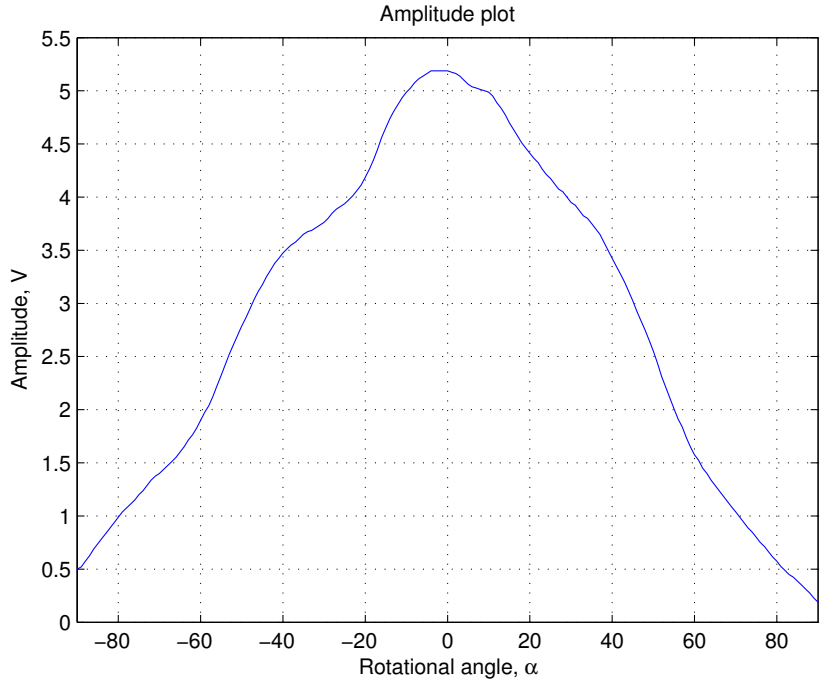

Figure 8.3: Amplitude vs rotational angle

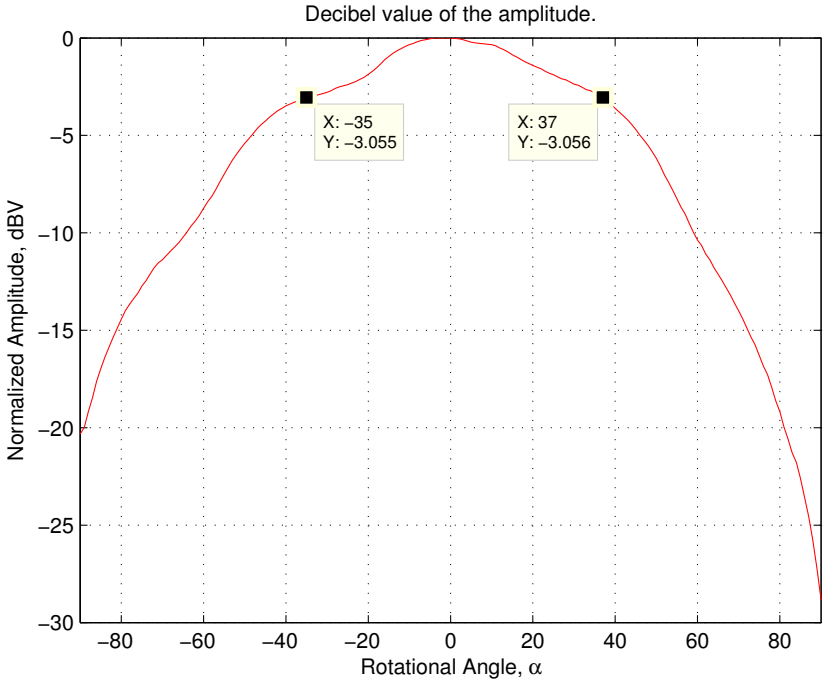

Figure 8.4: Amplitude dB plot

Figure 8.3 shows the amplitude of the sound signal (in voltage, V) as a function of the rotational angle α. As expected the maximum amplitude is achieved at $\alpha = 0°$. The amplitude reduces as we rotate the transducer, which is expected since the rotational angle α is proportional to beam angle θ_p. The distance to receiver increases as well by rotating the transducer. However the reduction of the amplitude has to do with the directivity index of the transducer and the distance between transducer and hydrophone.

Figure 8.4 shows the normalized amplitude in dB plot. It is marked in the figure where the -3dB point is. It appears at the rotational angles $\alpha = 37°$ and $\alpha = -35°$. Since the α has an error of $1°$, I will consider the -3dB point to appear at $\alpha = 36°$.

Beamwidth calculation

Now going back to the beamwidth problem from chapter 6. The geometry is illustrated in Figure 6.3 in chapter 6. It is mentioned there that the beam angle θ_p is half the beamwidth angle β:

$$a_{36°} = r \times \sin 36° = 3.53cm$$

$$b_{36°} = r \times \cos 36° = 4.85cm$$

$$x'_{36°} = D - b_{36°} = 22.55cm$$

$$x_{36°} = \sqrt{a_{36°}^2 + x_{36°}'^2} = 22.82cm$$

$$\sin\phi = \frac{a_{36°}}{x_{36°}} \rightarrow \phi = 8.9°$$

$$\frac{\beta}{2} = \theta_p = \alpha + \phi = 36° + 8.9° = 44.9° \rightarrow \beta = 89.8° \tag{8.1}$$

This means that our signal has a mainlobe of $\beta = 89.8°$ (in radians, $\beta = 1.57rad$), and the theory of omni-directional signal is not the case. However this can be compared with the beampattern of the transducer.

Finding the effective element size, d_{eff}

There is a possibility that explains why my signal is not a omni-directional signal. Since my transducer is only connected to one stripe and the other stripes are unconnected and since they are very closed to each other, there is some possibility that the extra energy is coming from the neighbouring

unconnected elements. When the element vibrates, it may vibrate the neighboring elements as well. If we take this theory further, we can calculate the effective element size d_{eff} of the transducer:

$$\sin\beta = \frac{\lambda}{d_{eff}} \rightarrow d_{eff} = \frac{\lambda}{\sin\beta} = \frac{1.488cm}{\sin 1.57} = 1.488cm \rightarrow d_{eff} \approx \lambda \tag{8.2}$$

This gives the interfering element size d_{int} from the neighboring elements as:

$$d_{int} = d_{eff} - d_{element} = 1.488cm - 1cm = 0.488cm \tag{8.3}$$

Assuming that interference is the same on both sides, we get the interference from each element of 0.244 cm.

8.1.2 Beampattern comparison

The effective element size theory can be further studied by simulating or comparing different beampatterns for the transducer with different element size. In this section I will compare those patterns with my measured amplitude dB plot, and conclude that the effective element size theory is more probable than beampattern theory.

In *Selfridge, Kino and Khuri-Yakub (1980)[?]*, it is stated that the angular response pattern of a single element is of the form:

$$p = p_0 \frac{\sin\frac{\pi d}{\lambda} \times \sin\theta_p}{\frac{\pi d}{\lambda} \times \sin\theta_p} \tag{8.4}$$

In my simulations I have used that $p_0 = 1$. In the same article *Selfridge, Kino and Khuri-Yakub (1980)[?]* uses an extra term of $\cos\theta_p$ to narrow the beampattern. They used Rayleigh-Sommerfield diffraction formula, which gave them this result:

$$p(r,\theta_p) = \frac{p_0 d}{j(\lambda)^{1/2}} e^{2j\pi r/\lambda} \times \frac{\sin\frac{\pi d}{\lambda} \times \sin\theta_p}{\frac{\pi d}{\lambda} \times \sin\theta_p} \times \cos\theta_p \tag{8.5}$$

This is also stated in *Johnson and Dudgeon p. 37 (1993) [?]. Johnson and Dudgeon p. 63 (1993) [?]* defines a linear aperture function as:

$$W = \frac{\sin k_x d/2}{k_x/2} \tag{8.6}$$

Where $k_x = k \times \sin\theta_p = \frac{2\pi}{\lambda} \times \sin\theta_p$. With some discussion with my supervisor *Sverre Holm*, I was motivated to compare with another pattern described in Equation 8.7. This pattern gets the extra term of $\frac{1+\cos\theta_p}{2}$ instead of $\cos\theta_p$ in Equation 8.5. This pattern is supposed to lie in between of patterns in Equation 8.4 and in Equation 8.5. My supervisor couldn't find any reference for this formula but he remembered it from his earlier works. However this pattern was simulated just because I was curious.

$$b(\theta_p) = \frac{\sin\frac{\pi d}{\lambda} \times \sin\theta_p}{\frac{\pi d}{\lambda} \times \sin\theta_p} \times \frac{1+\cos\theta_p}{2} \tag{8.7}$$

As seen in Figure 8.5, the measured amplitude is close to the first beampattern in Equation 8.4, but still Equation 8.4 is a bit wider (Equation 8.4 is equal to Equation 8.6, and thus they have the same pattern in Figure 8.5. That's why the Equation 8.4 is not visible). The reason why my measured amplitude doesn't get any zero points is because I'm transmitting a pulsed signal, and that's obvious that I will not get any zeros in my amplitude plot. Since the theoretical pattern is wider, and the measured amplitude does not fully follow this pattern, thus the theory of effective element size is more probable in my case. In the Figure 8.6 I have plotted the patterns in different element size, and tried to study the behaviour of the theoretical patterns. The patterns gets narrower and equal to each other as I increase the element size. This does not satisfy the theory of effective element size, but is an indicator that for some element size the amplitude plot is almost equal to the theoretical pattern in Equation 8.4.

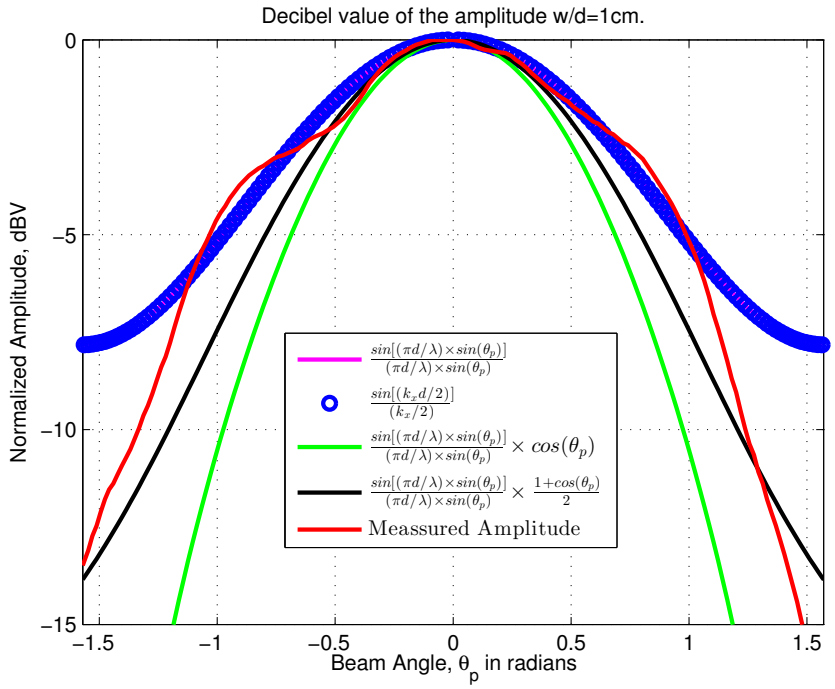

Figure 8.5: Different beampatterns with element size $d = 1cm$. The one with magneta color is the pattern in Equation 8.4, the green is from Equation 8.5, the black is from Equation 8.7, the dots are from Equation 8.6 and the red one is the measured amplitude in dbV.

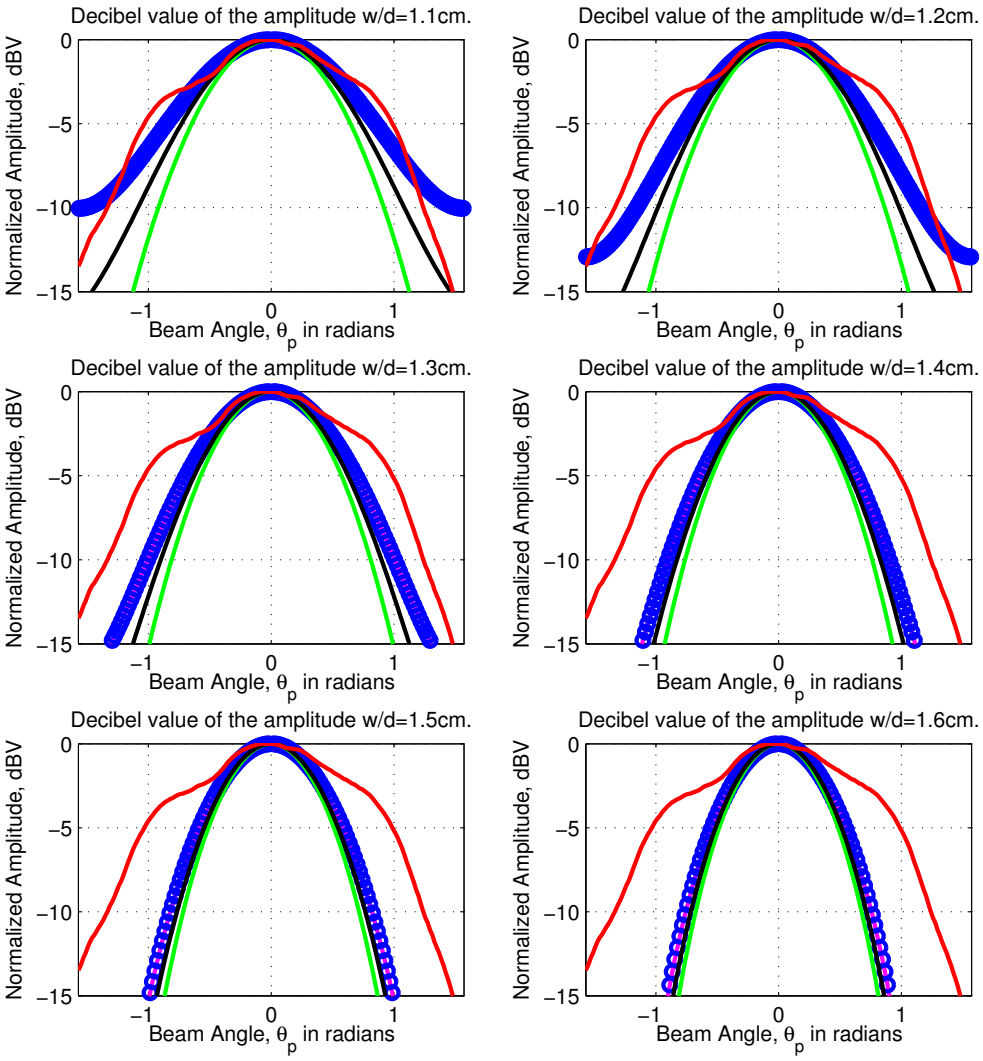

Figure 8.6: Different beampatterns with respectively element size $d = 1.1cm$, $d = 1.2cm$, $d = 1.3cm$, $d = 1.4cm$, $d = 1.5cm$ and $d = 1.6cm$

8.1.3 Instrumental delay

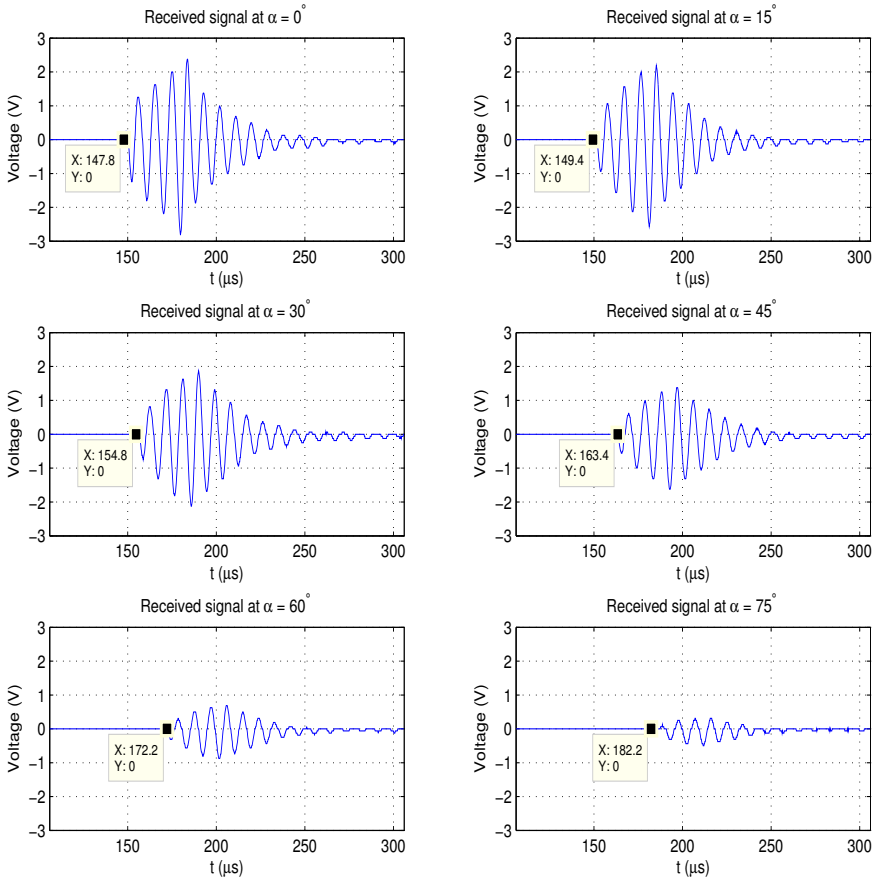

Figure 8.7: Signals captured in different rotational angle

Instrumental delay in this case is the total instrumental delay from all instruments used. Equipments such as the generator, transducer and hydrophone have some sort of delays. This is important when I have to calculate the sound velocity in experiment IV.

I have chosen to investigate the instrumental delay at some angles, and as shown in Figure 8.7, I have marked their time of arrival T at the hydrophone. Instrumental delay is given as ΔT:

$$T_\alpha = t_\alpha + \Delta T_\alpha \tag{8.8}$$

Where $t_\alpha = \frac{x_\alpha}{c}$, T_α is the total time registered in the oscilloscope and ΔT_α is the instrumental delay. From Equation 8.8 I get the following equation for the instrumental delay:

$$\Delta T_\alpha = T_\alpha - t_\alpha \tag{8.9}$$

By taking T_α from Figure 8.7 and x_α from Table 8.1, I get the following values for ΔT_α:

α	$T_\alpha(\mu s)$	$t_\alpha(\mu s)$	$\Delta T_\alpha(\mu s)$
0°	147.8	143.8	4
15°	149.4	145.6	3.8
30°	154.8	150.5	4.3
45°	163.4	158.2	5.2
60°	172.2	167.7	4.5
75°	182.2	178	4.2

Table 8.1: Instrumenta delay on different rotational angles

From this it seems that the instrumental delay is about $4\mu s$, but I will calculate the instrumental delay by taking the means of these values. The instrumental delay becomes:

$$\Delta T = \frac{\Delta T_{0^\circ} + \Delta T_{15^\circ} + \Delta T_{30^\circ} + \Delta T_{45^\circ} + \Delta T_{60^\circ} + \Delta T_{75^\circ}}{6} = 4.33\mu s \tag{8.10}$$

8.2 Experiment IV - Back experiment

This experiment was done by rotating the transducer from 85° to 275° with an interval of 1°. In this experiment I had to increase the amplitude on the input signal, since the signal got weaker when operating in this region of rotation. I could not increase the amplitude much more because of the limitations on the amplifier.

Figure 8.8 shows the plot which was obtained when the experiment was finished, and Figure 8.9 shows dB value plot at every rotational angle. The amplitude plot in V and dBV is shown in Figure 8.13 and Figure 8.14. From Figure 8.9 and Figure 8.13 it is shown that the signal is received upto $\alpha = 120^\circ$. From $\alpha = 120^\circ$ to $\alpha = 240^\circ$ the signal could not be received or not could not be distinguished from the noise. This is further confirmed in Figure 8.10.

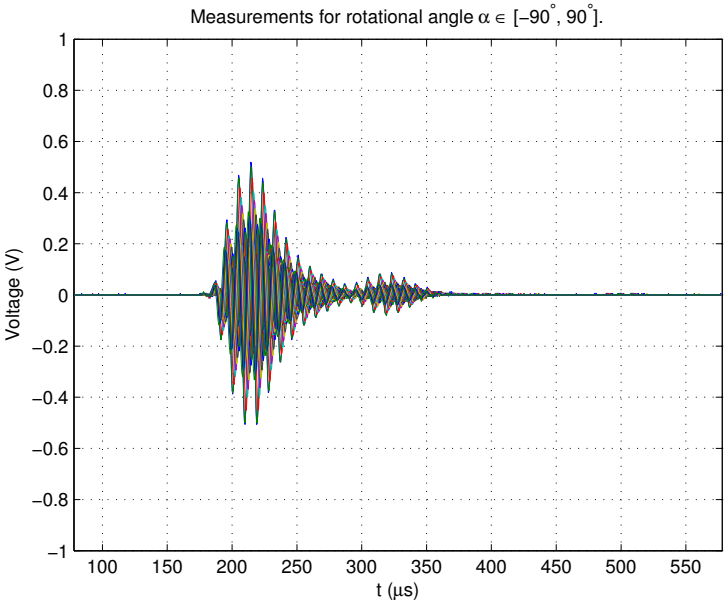

Figure 8.8: Signal captured by the oscilloscope

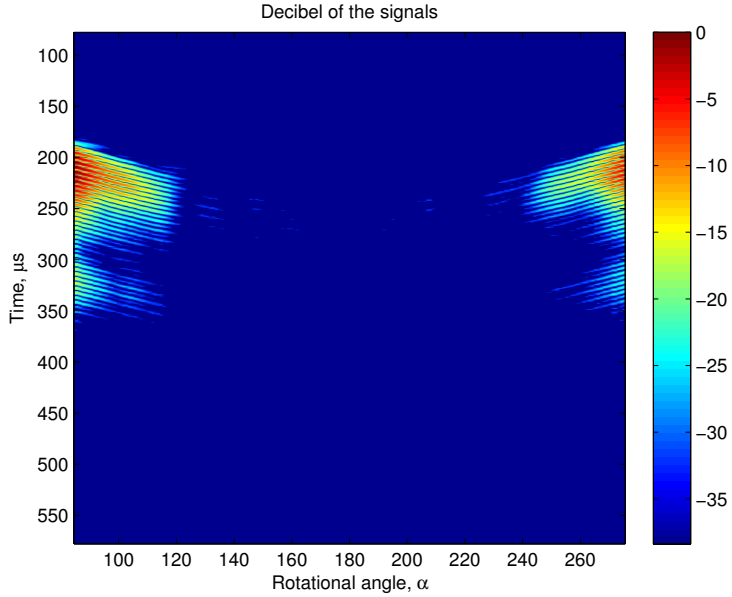

Figure 8.9: Signal in dB

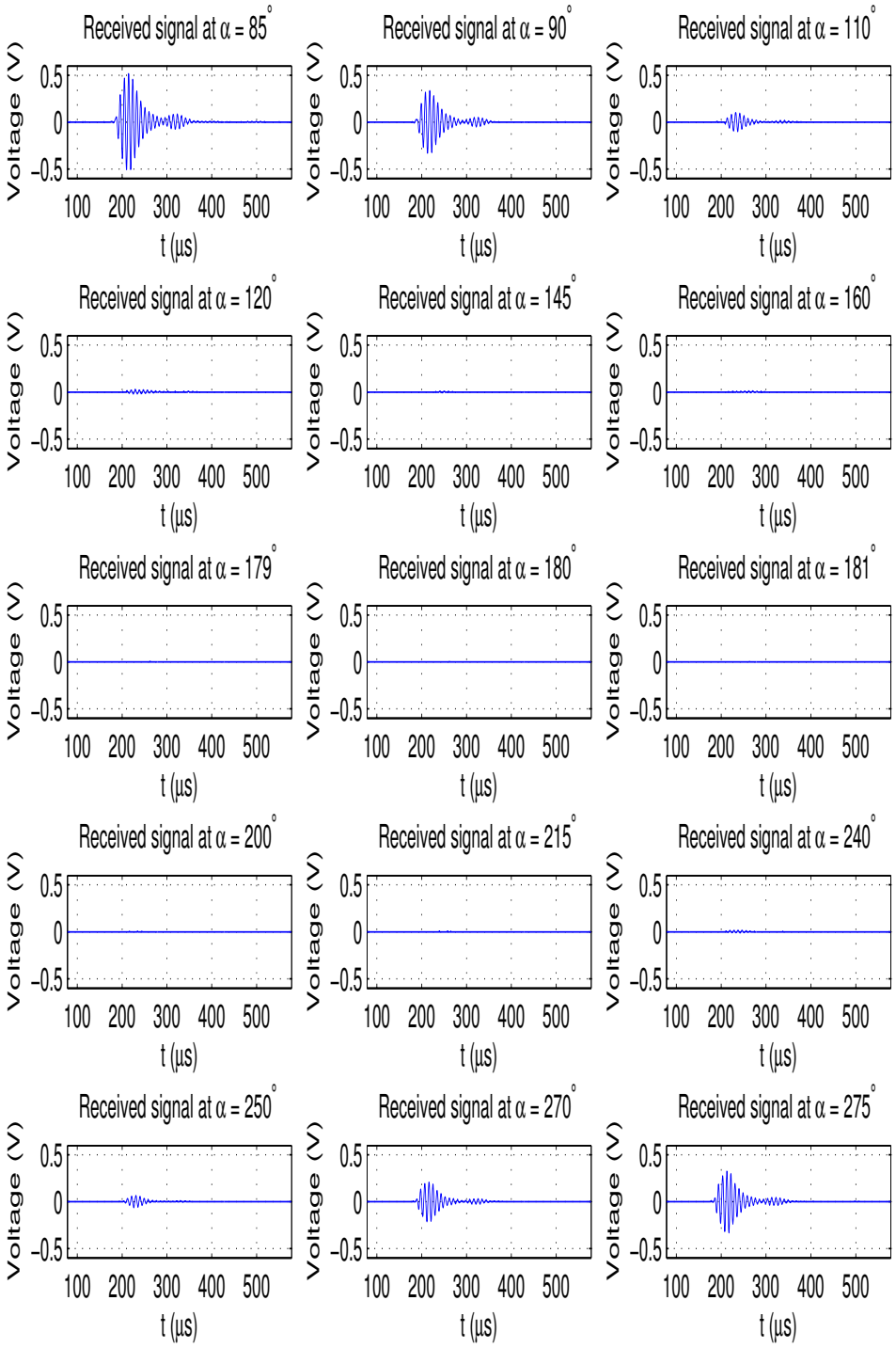
Received signal at α = 85°
Received signal at α = 90°
Received signal at α = 110°
Received signal at α = 120°
Received signal at α = 145°
Received signal at α = 160°
Received signal at α = 179°
Received signal at α = 180°
Received signal at α = 181°
Received signal at α = 200°
Received signal at α = 215°
Received signal at α = 240°
Received signal at α = 250°
Received signal at α = 270°
Received signal at α = 275°
Voltage (V)
0.5
0
−0.5
100 200 300 400 500
t (μs)

Figure 8.10

Figure 8.10 shows the signal in rotational angles 85°, 90°, 110°, 120°, 145°, 160°, 179°, 180°, 181°, 200°, 215°, 240°, 250°, 270° and 275°.

It becomes more clear now that I have no signal at 180°. This can have many reasons and some of them are discussed in Chapter 9 (conclusion and discussion). However, the signal seems to be "drowned" in noise. It has to be noted that I have reduced the noise on my figures, thus the signal does not appear. That's alright since the signal is too small, thus I can say that I'm not receiving any signal at this point. Figure 8.10 also confirms that the signal seems to be totally reduced after 120°.

If I further study the signal from 85° to 90° and compare it with experiment III, then it is (as expected) higher in amplitude, but (not expected) reaches the hydrophone earlier than in experiment III. The reason behind this can be many, but some of them are discussed in Chapter 9 (conclusion and discussion). Figure 8.11 shows the signal from experiment III and Figure 8.12 shows the signal from experiment IV:

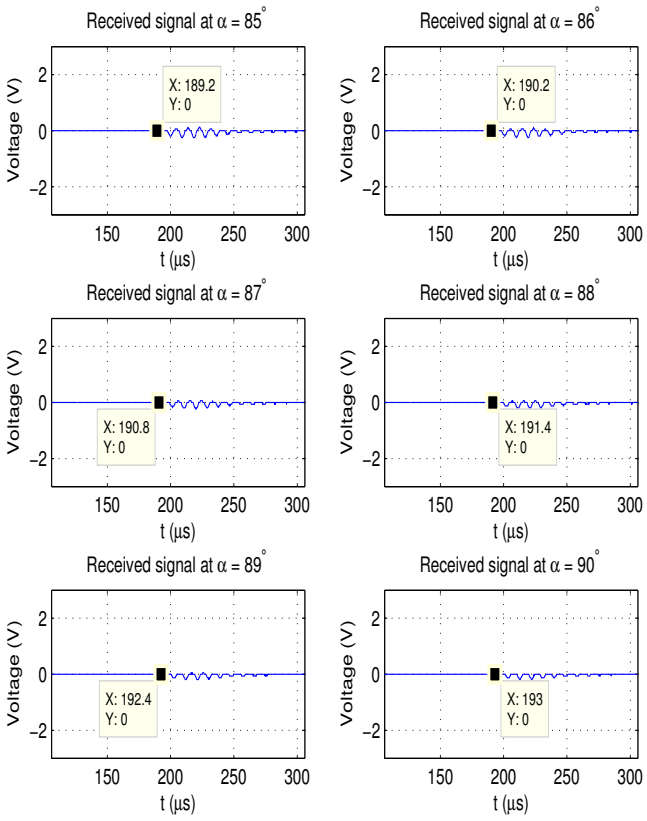

Figure 8.11: Signal output for experiment III

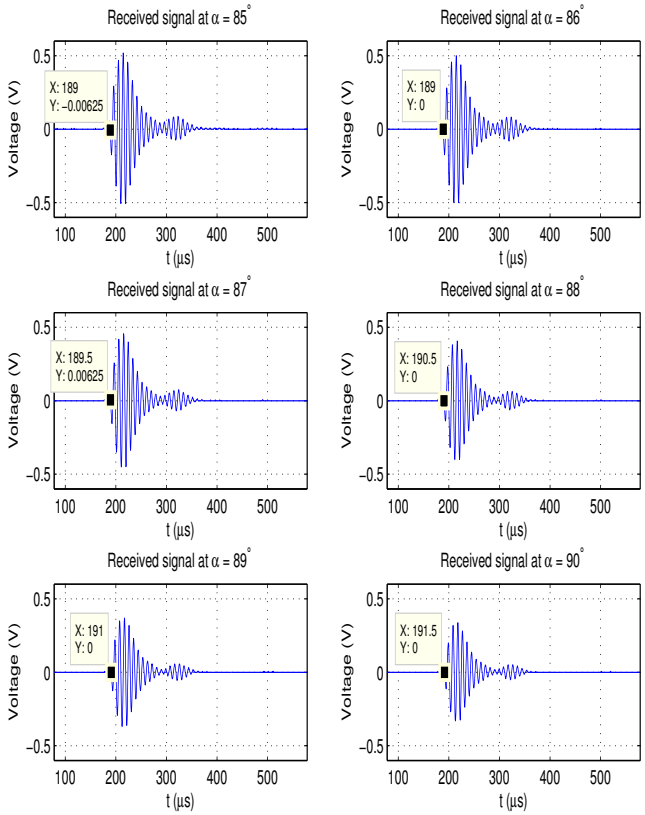

Figure 8.12: Signal output for experiment IV

8.2.1 Amplitude plot and comparison from experiment III

As mentioned earlier, Figure 8.13 and Figure 8.14 are amplitude plots of experiment IV. As it is shown, the amplitude is almost $0V$ after about $\alpha = 120°$ and before about $\alpha = 240°$.

One thing I'm very interested in studying is how to compensate amplitudes of experiment III and experiment IV. As mentioned the signal input voltage in experiment IV is higher than in experiment III. To study this I have plotted the amplitude on both experiments in Figure 8.15, and then compensated for the amplitude difference at $\alpha = 85°$ to $\alpha = 90°$ and the same on the other side. That is why I had to do experiment IV from $\alpha = 85°$ to $\alpha = 275°$ and not from $\alpha = 90°$ to $270°$. The compensated amplitude plot of the whole transducer from $\alpha = 0°$ to $\alpha = 359°$ is shown in Figure 8.16.

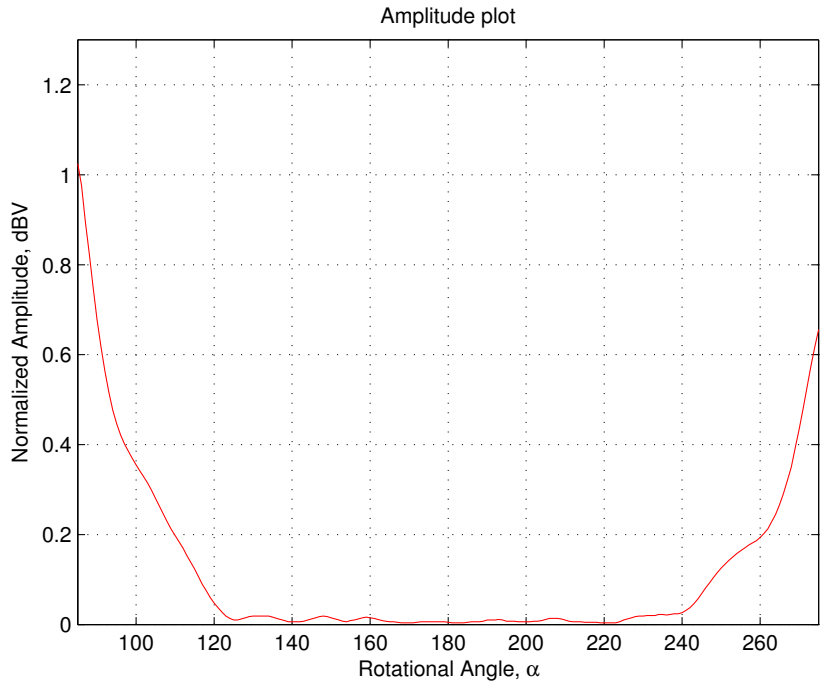

Figure 8.13: Amplitude vs rotational angle

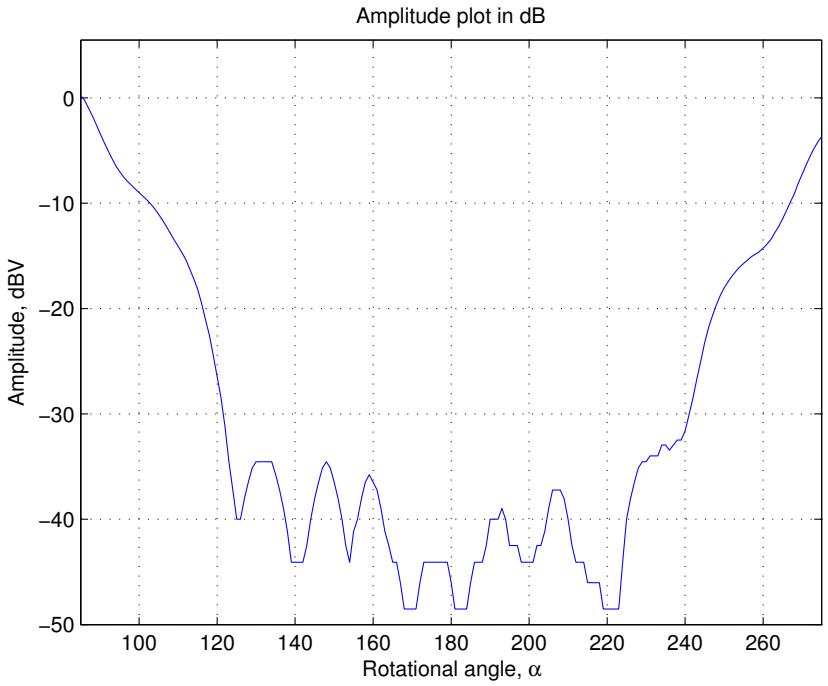

Figure 8.14: Amplitude vs rotational angle in dB

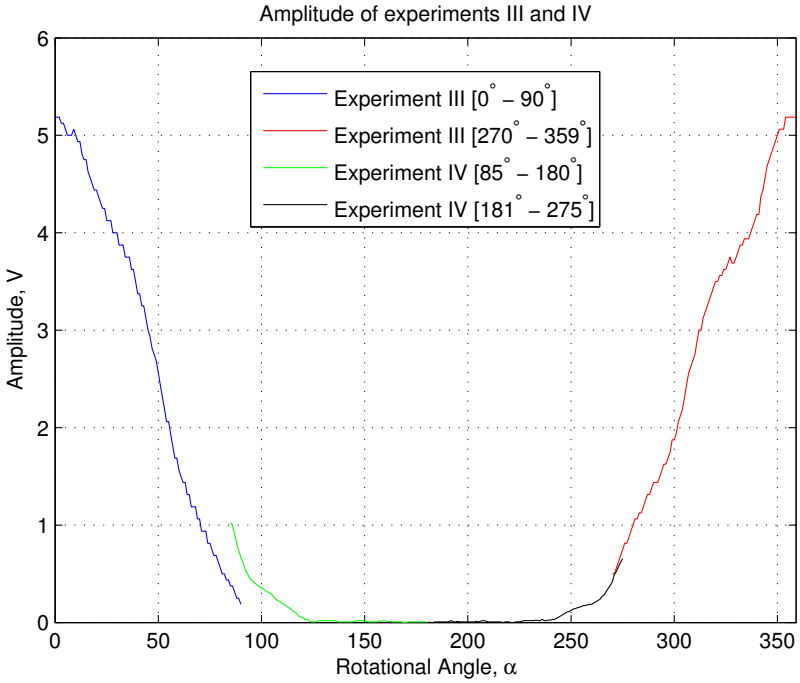

Figure 8.15: Amplitude plot of experiment III and IV

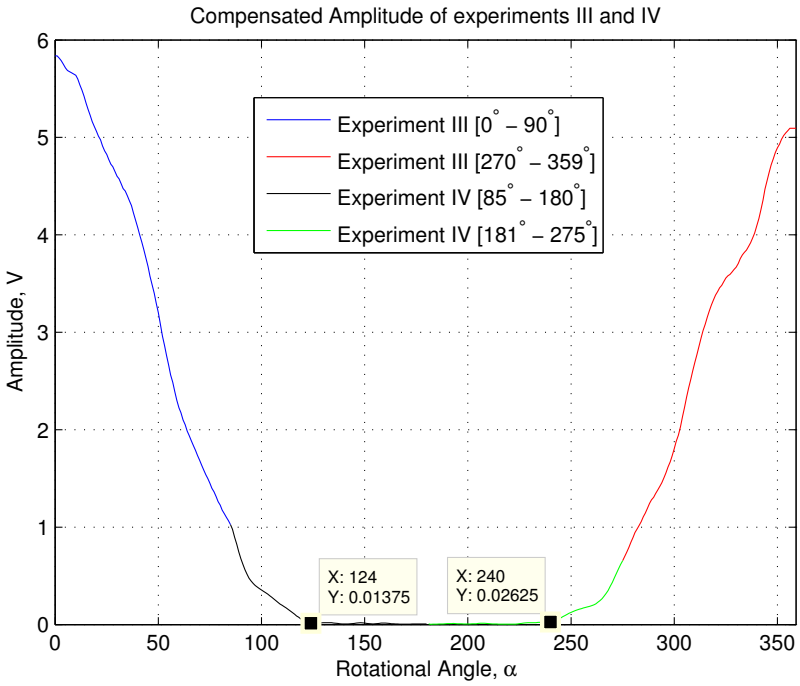

Figure 8.16: Compesated amplitude plot

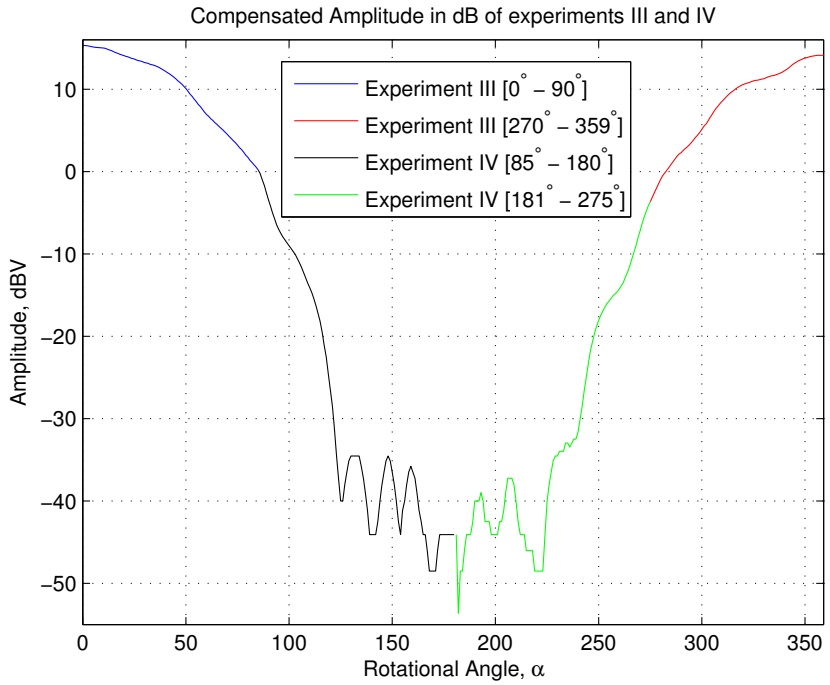

Figure 8.17: Compensated amplitude plot in dB

8.3 Sound velocity profile for $\alpha \in [\alpha_{tangent}, 360° - \alpha_{tangent}]$

In this section I will calculate the sound velocity when the transducer is not transmitting the sound signal "direct" to the hydrophone. To do so I have to calculate the distance from the element to the receiver at some given rotational angle α. It was found in chapter 6 that the distance between transducer and receiver (when the rotational angle was $\alpha_{tangent} = 77.36° \approx 77°$) was $x_{\alpha_{tangent}} = 26.7cm$. To calculate the distance by rotating the transducer by α is given as:

$$x_\alpha = \underbrace{2\pi r\left(\frac{\alpha - \alpha_{tangent}}{360°}\right)}_{\bar{x_\alpha}} + x_{\alpha_{tangent}}$$

Since the signal is readable for upto $\alpha = 120°$ I will only calculate the distance upto that point. The distance $\bar{x_\alpha}$ is the circular bow on the transducer. The distances is given in Table 8.2

α	$\bar{x_\alpha}(cm)$	$x_\alpha(cm)$
85°	0.84	27.5
90°	1.36	28.06
95°	1.88	28.58
100°	2.4	29.1
105°	2.93	29.63
110°	3.46	30.16
115°	3.98	30.68
120°	4.5	31.2

Table 8.2: Distance to receiver

From Figure 8.11 and Figure 8.12 I know the received time is incorrect in experiment IV compared to in experiment III. Therefor I am going to calculate the velocity from a given rotational angle α to $\alpha = 90°$. For that I need to know the circular bow of that rotational angle α to $\alpha = 90°$. This is given as:

$$\bar{x_{\alpha-90°}} = 2\pi r \frac{\alpha - 90°}{360°}$$

Figure 8.18 shows the received signals at different times at rotational angles, $\alpha = [95°, 100°, 105°, 110°, 115°, 120°]$. The received time at $\alpha = 90°$ are shown in Figure 8.12. The sound velocity is calculated as:

$$\bar{t_{\alpha-90°}} = T_\alpha - T_{90°} = T_\alpha - 191.5\mu s$$

$$c_\alpha = \frac{\bar{x_{\alpha-90°}}}{\bar{t_{\alpha-90°}}}$$

The result is given in Table 8.3:

α	$\bar{x_{\alpha-90°}}(cm)$	$\bar{t_{\alpha-90°}}(\mu s)$	$c_\alpha(m/s)$
95°	0.52	4	1300
100°	1.05	8	1312
105°	1.57	11.5	1365
110°	2.09	16	1306
115°	2.62	20	1310
120°	3.14	22.5	1395

Table 8.3: Sound velocity for experiment IV

It seems like the sound velocity is almost constant around $1300m/s$ - $1400m/s$.

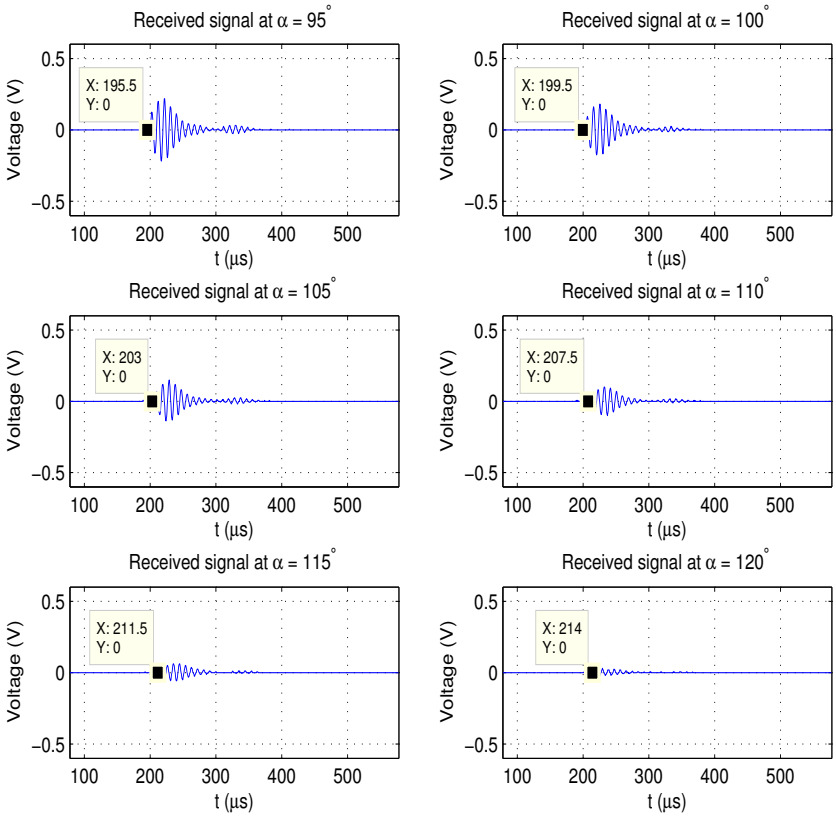

Figure 8.18: Signal output for experiment IV

Part IV

Conclusion

Chapter 9

Conclusion and discussion

9.1 Conclusion

As seen on the results in experiment IV, the signal is obtained and received when the rotational angle is within $\alpha \in [-120°, 120°]$. When the rotational angle is outside this boundary the signal seems to be "drowned" in noise and is unable to read on the oscilloscope. There are two ways to conclude why this is the case, and both may be proportional to each other.

The first way is to compare with Figure 9.1 and Figure 9.2 (*made by my supervisor Sverre Holm, code based on Duda and Martens (1998)[**?**] and referenced from Morse and Ingard (1968)[**?**]*). These are the theoretical models for human listening. The signal response is plotted as a function of angles with different $\mu = ka$ values. μ is the normalized frequency, where $k = \frac{2\pi}{\lambda}$ and a = radius of the head/sphere. The normalized frequency μ in this thesis is $\mu = ka = 25.34 \approx 25$.

By first studying Figure 9.1, I can see that my signal should be somewhere between the green and the black plot. The green starts to oscillate (or has it ripples) around $140°$, and a $\mu = 20$. Figure 9.2 is more interesting and important in my case, since it describes the decrease of the response when $\mu = 25$. From Figure 9.2 it can be seen that the signal response falls with about $17 - 18db$, and in my experiments the signal amplitude falls with about $50 - 55db$. The most important thing is to see that the response starts to oscillate (or has it ripples) around $120°$, which is very close to my results.

The second way to look at the result is by the theory given in Chapter 4. In my thesis the background is indicated either by noise background or reverberation background. However, in both cases the signal/echo level SL is larger than the noise or reverberation level NL or RL, upto a range R_n or R_r. As familiar, the source to receiver range increases by rotating the transducer towards $\alpha = 180°$. So the signal/echo level SL is a function of range as well as for α. From Chapter 4 it is known that for some range R_r or R_n the signal/echo level SL equals the reverberation- or noise level RL or NL. And for ranges larger than R_r or R_n the signal gets smaller than the background,

and is impossible to distinguish from the background. In my experiments, there has to be a point right after $\alpha = 120°$ where the signal/echo level SL equals the background level, and therefore is impossible to distinguish from the background source.

However, both of these cases concludes with that my results are pretty good, and the signal is not "achievable" after $\alpha = 120°$.

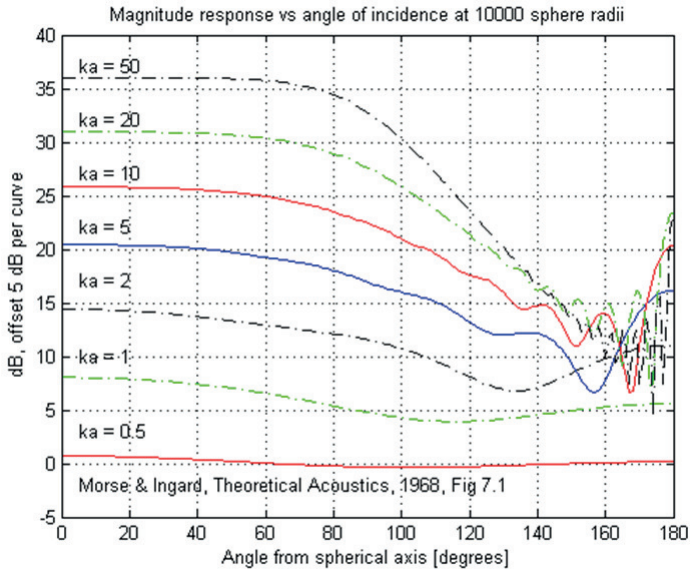

Figure 9.1: Signal response in dB vs angle for different ka values

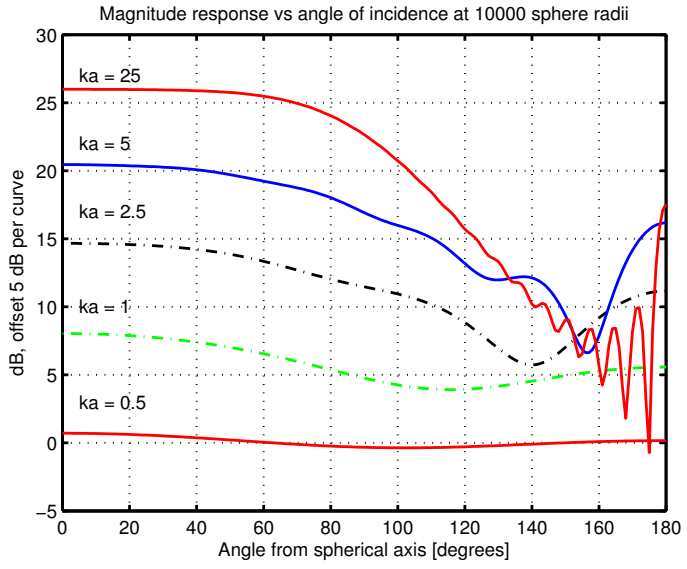

Figure 9.2: Signal response in dB vs angle for different $kavalues$, and especially for $ka = 25$

9.1.1 Sound propagation path

In chapter 6 I had given some cases for how the sound signal propagates in two different α regions. After the results in experiment III and IV, I can conclude that for $\alpha \in [-\alpha_{tangent}, \alpha_{tangent}]$ the sound waves travels directly towards the hydrophone, hence case I is correct and case II is uncorrect. When I measured the instrumental delay I assumed that case I was correct, and that gave me almost identically delays at different angles, and that proves my assumption was correct.

For $\alpha \in [\alpha_{tangent}, 360° - \alpha_{tangent}]$ case III seems to be correct. Since the measuring of sound velocity in experiment IV gave me almost identically sound velocities in all angles. The sound velocities in this region seems to be smaller than sound velocity in water, thus I can conclude that the sound is travelling along the surface of the transducer until it reaches the tangent point and then travels directly towards the hydrophone. It is said in *Selfridge, Kino and Khuri-Yakub (1980)*[**?**] that: *In typical applications, the transducer element is separated from the water medium by a thin membrance or by a rubberlike material of the same impedance as water.* This means that the sound velocity has to be the same if the density of the material is the same as water. The reason of getting slower sound velocity are many, and they are discussed in next section.

9.2 Discussion

Working on this thesis was very complicated and challenging. In this section I'm going to discuss some factors which may have played some part in "bad" measurement results in the experiments. This factors are important to take in consideration when reading this thesis.

- Deviation in geometry

  The hydrophone may have not been placed in front of the transducer, in both horizonal or vertical plane.

  Since experiments was done in different days and I had to move the transducer after every experiment, thus the geometry may not be same in every experiment. That could have been the reason why sound wave reached earlier to the receiver in experiment IV.

- Inexperienced in measurements
- Time display in the oscilloscope may have some deviation from real time.
- Rotation by $1°$ may not rotate $1°$ but with some deviation.
- The radius of the transducer may be different than measured.
- Leakage of water in the tank may give wrong positions for the transducer according to the amount of water in the tank.

- Air bubbles occured on the surface of the transducer and hydrophone while doing the experiments. This gave some time delay and reduction of amplitude on the received signal. When the air bubbles was cleaned, the signal got bigger in amplitude and it was impossible to compare it with other measurements and the experiment had to be done over again.
- Since the experiments was done in different days and we don't have some cleaning system mounted on the tank, the water may have been dirty. Some of the dirt may have been placed at the surface of both transducer and hydrophone.
- Air bubbles and dirt on transducer may have been the reason why sound velocity along the surface of the transducer was lower than sound velocity in water.
- Temperature may have also changed as the days past.
- As seen from all experiments, the received signal has some ripples in the end of the signal. This could have been caused by diffraction of the sound signal by the hydrophone's shape or by reflection and scattering caused by the hydrophone and the probe it is mounted on.
- The result could have been better if I had sent a sound signal with higher amplitude, or sent with lower frequency. Both increasing the amplitude and decreasing the frequency was impossible in this thesis, because of the limitations on the transducer and the JBL amplifier.

9.3 Future work

- Do experiment III and experiment IV over again. Since I have now got more experienced in measuring in the tank than before.
- Transmitting less or more pulse periods.
- Do the experiment with lower μ value, better if the μ value is comparable for humans as well. For example with a head of radius $a = 6cm$, and a frequency range of $20 - 20,000Hz$, the μ value for human head is around 0.02 and 21.66. For getting in this region I'll have to reduce my frequency input, and for doing that I have to change my transducer to another one that matches these limitations. This wasn't easy in my case, since there was no choose and throw concept about the transducer. First of all, I had to take the one that was available. The second one, I neeed a commercial Simrad transducer for this experiment. A transducer with high frequency, since the water tank is too small. *Kongsberg Maritime AS* had another transducer available, but that one had to low μ value (Operated in a frequencies about $20kHz$-$30kHz$). It would have been difficult to do measurements with that transducer.

- Do the experiment with higher amplitude, so the signal level can be separated from the background when the transducer is rotated 180°. For tis I'll have to change the audio JBL amplifier with one that fits these limitations.
- Inserting small fishes in the tank and receiving with a circular transducer. Check if it's possible to receive the signal if the transducer element is 180° to the fish.

Part V

Appendix

Appendix A

All the simulation and programming in this thesis has been done in Matlab software. There has been written a simulation code for the tank by professor Svein Bøe in Matlab which was used and modified during the experiments (I haven't attached this on here, but can be shown if needed). Three of the experiments is done with my co-student Asle Tangen (had another master thesis than me), but the processing of data afterwards is done individually.

Below is my matlab code that I programmed to process my data from all experiments:

Matlab Code

Code for experiment I:

```
% Experiment I

H = figure;

load('x27.mat')
Vpp1 = max(S)-min(S);
plot(z, Vpp1);
hold on
axis tight
title('Amplitude variation in height with spesific
    angles')
xlabel('Height, mm')
ylabel('Amplitude, V')
grid on
set(gca,'xdir','reverse');

clear S

load('x34.mat')
Vpp2 = max(S)-min(S);
plot(z, Vpp2, 'r');
```

```
21 axis tight
22 % title('34 grader')
23 xlabel('Hoyde i mm')
24 ylabel('Spenning i V')
25 grid on
26 set(gca,'xdir','reverse');
27
28 clear S
29
30 load('x41.mat')
31 Vpp3 = max(S)-min(S);
32 plot(z, Vpp3, 'g');
33 axis tight
34 % title('34 grader')
35 xlabel('Hoyde i mm')
36 ylabel('Spenning i V')
37 grid on
38 set(gca,'xdir','reverse');
39
40 clear S
41
42 load('x48.mat')
43 Vpp4 = max(S)-min(S);
44 plot(z, Vpp4, 'k');
45 axis tight
46 % title('34 grader')
47 xlabel('Hoyde i mm')
48 ylabel('Spenning i V')
49 grid on
50 set(gca,'xdir','reverse');
51
52 clear S
53
54 load('x55.mat')
55 Vpp5 = max(S)-min(S);
56 plot(z, Vpp5, 'c');
57 axis tight
58 % title('34 grader')
59 xlabel('Hoyde i mm')
60 ylabel('Spenning i V')
61 grid on
62 set(gca,'xdir','reverse');
63
64 clear S
65
66 load('x62.mat')
67 Vpp6 = max(S)-min(S);
68 plot(z, Vpp6, 'm');
```

```
69 axis tight
70 % title('34 grader')
71 xlabel('Hoyde i mm')
72 ylabel('Spenning i V')
73 grid on
74 set(gca,'xdir','reverse');
75
76 clear S
77
78 load('x69.mat')
79 Vpp7 = max(S)-min(S);
80 plot(z, Vpp7, '*');
81 axis tight
82 % title('34 grader')
83 xlabel('Hoyde i mm')
84 ylabel('Spenning i V')
85 grid on
86 set(gca,'xdir','reverse');
87
88 clear S
89
90 load('x76.mat')
91 Vpp8 = max(S)-min(S);
92 plot(z, Vpp8, '.');
93 axis tight
94 % title('34 grader')
95 xlabel('Hoyde i mm')
96 ylabel('Spenning i V')
97 grid on
98 set(gca,'xdir','reverse');
99
100 clear S
101
102 load('x83.mat')
103 Vpp9 = max(S)-min(S);
104 plot(z, Vpp9, 's');
105 axis tight
106 % title('34 grader')
107 xlabel('Height, mm')
108 ylabel('Amplitude, V')
109 grid on
110 set(gca,'xdir','reverse');
111
112 clear S
113
114 load('x90.mat')
115 Vpp10 = max(S)-min(S);
116 plot(z, Vpp10, 'o');
```

```
117 axis tight
118 % title('34 grader')
119 xlabel('Height, mm')
120 ylabel('Amplitude, V')
121 grid on
122 set(gca,'xdir','reverse');
123
124 clear S
125
126 load('x97.mat')
127 Vpp11 = max(S)-min(S);
128 plot(z, Vpp11, 'd');
129 axis tight
130 % title('34 grader')
131 xlabel('Height, mm')
132 ylabel('Amplitude, V')
133 grid on
134 set(gca,'xdir','reverse');
135 legend('-35{^\circ}', '-28{^\circ}','-21{^\circ}','
    -14{^\circ}','-7{^\circ}','0{^\circ}','7{^\circ}','
    14{^\circ}','21{^\circ}','28{^\circ}','35{^\circ}')
136
137
138 Y = figure;
139
140 Vpp = [Vpp1' Vpp2' Vpp3' Vpp4' Vpp5' Vpp6' Vpp7' Vpp8'
     Vpp9' Vpp10' Vpp11'];
141
142 imagesc(theta,x, db(Vpp))
143 title('Amplitude in dB as a function of angle and
    height')
144
145 xlabel('Angle, {^\circ}')
146 ylabel('Height, mm')
147    hd= colorbar;
148    set(get(hd,'ylabel'),'String','Amplitude, dBV', '
       Rotation',-90.0);
149
150 W = figure;
151
152 surf(theta, x, db(Vpp))
153 title('3D plot of Amplitude in dB as a function of
    angle and height')
154 xlabel('Angle, {^\circ}')
155 Xlab=get(gca,'xlabel');
156 set(Xlab,'rotation',20)
157 ylabel('Height, mm')
158 Ylab=get(gca,'ylabel');
```

```
159 set(Ylab,'rotation',-25)
160    hd= colorbar;
161    set(get(hd,'ylabel'),'String','Amplitude, dBV', '
       Rotation',-90.0);
162
163
164 saveas(H, 'amplitude_hoyde', 'epsc')
165 saveas(Y,'hoyde_vinkelAmplitude', 'epsc')
166 saveas(W, 'hoyde_vinkelAmplitude3D','epsc')
```

```
1  theta = [-35:7:35];
2
3  load('x27.mat');
4  S1 = S(:,14);
5  Vpp_S1 = max(S1)-min(S1);
6
7  load('x34.mat');
8  S2 = S(:,14);
9  Vpp_S2 = max(S2)-min(S2);
10
11 load('x41.mat');
12 S3 = S(:,14);
13 Vpp_S3 = max(S3)-min(S3);
14
15 load('x48.mat');
16 S4 = S(:,14);
17 Vpp_S4 = max(S4)-min(S4);
18
19 load('x55.mat');
20 S5 = S(:,14);
21 Vpp_S5 = max(S5)-min(S5);
22
23 load('x62.mat');
24 S6 = S(:,14);
25 Vpp_S6 = max(S6)-min(S6);
26
27 load('x69.mat');
28 S7 = S(:,14);
29 Vpp_S7 = max(S7)-min(S7);
30
31 load('x76.mat');
32 S8 = S(:,14);
33 Vpp_S8 = max(S8)-min(S8);
34
35 load('x83.mat');
36 S9 = S(:,14);
37 Vpp_S9 = max(S9)-min(S9);
38
```

```
load('x90.mat');
S10 = S(:,14);
Vpp_S10 = max(S10)-min(S10);

load('x97.mat');
S11 = S(:,14);
Vpp_S11 = max(S11)-min(S11);

Vpp = [Vpp_S1 Vpp_S2 Vpp_S3 Vpp_S4 Vpp_S5 Vpp_S6
    Vpp_S7 Vpp_S8 Vpp_S9 Vpp_S10 Vpp_S11];

plot(theta,smooth(Vpp))
F = figure, plot(theta, smooth(db(Vpp)))
grid on
title('Amplitude when receiver position is constant,
    and by rotating transducer')
xlabel('angle,{^\circ}')
ylabel('log of Amplitude, dBV')

saveas(F, 'Amplitude_angle_height960', 'epsc')
```

Code for experiment II:

```


load('lydhast21_4cm.mat');
X1 = S;
load('lydhast41_4cm.mat');
X2 = S;

vpp1 = max(X1) - min(X1)
vpp2 = max(X2) - min(X2)


t1 = [67.2:0.2:267];
t2 = [204.8:0.2:404.6];



figure(1),plot(t1,X1)
axis([67 267 -5 5])
grid on
title('Hydrophone at a distance d = 21.4 cm.')
xlabel('t ({\mu}s)')
ylabel('Voltage (V)')

figure(2),plot(t2,X2,'r')
axis([204 405 -5 5])
```

```
title('Hydrophone at a distance d = 41.4 cm.')
xlabel('t ({\mu}s)')
ylabel('Voltage (V)')
grid on
```

Code for experiment III:

```
 load('exp_front181p_d21_4cm.mat');
 load('exp_front181p_d21_4cm_Vpp');

t1 = [106:0.2:305.8];
angle = [-90:1:90];

figure(1),plot(t1,S)
axis([106 306 -3 3])
grid on
title('Measurements for rotational angle {\alpha} {\in} [-90{^{\circ}}, 90{^{\circ}}]. ')
xlabel('t ({\mu}s)')
ylabel('Voltage (V)')

figure(2),plot(angle,smooth(db(Vpp/max(Vpp))),'r')
axis([-90 90 -30 0])
title('Decibel value of the amplitude.')
xlabel('Rotational Angle, {\alpha}')
ylabel('Normalized Amplitude, dBV')
grid on

figure(3),plot(angle,smooth(Vpp))
axis([-90 90 0 5.5])
title('Amplitude plot')
xlabel('Rotational Angle, {\alpha}')
ylabel('Amplitude, V')
grid on

figure(4), subplot(3,2,1);
plot(t1,S(:,91)), axis([106 306 -3 3])
grid on
title('Received signal at {\alpha} = 0{^{\circ}} ')
xlabel('t ({\mu}s)')
ylabel('Voltage (V)')

subplot(3,2,2),
plot(t1,S(:,106)), axis([106 306 -3 3])
grid on
title('Received signal at {\alpha} = 15{^{\circ}} ')
xlabel('t ({\mu}s)')
ylabel('Voltage (V)')
```

```
41
42 subplot(3,2,3);
43 plot(t1,S(:,121)), axis([106 306 -3 3])
44 grid on
45 title('Received signal at {\alpha} = 30{^{\circ}} ')
46 xlabel('t ({\mu}s)')
47 ylabel('Voltage (V)')
48
49 subplot(3,2,4);
50 plot(t1,S(:,136)), axis([106 306 -3 3])
51 grid on
52 title('Received signal at {\alpha} = 45{^{\circ}} ')
53 xlabel('t ({\mu}s)')
54 ylabel('Voltage (V)')
55
56 subplot(3,2,5);
57 plot(t1,S(:,151)), axis([106 306 -3 3])
58 grid on
59 title('Received signal at {\alpha} = 60{^{\circ}} ')
60 xlabel('t ({\mu}s)')
61 ylabel('Voltage (V)')
62
63 subplot(3,2,6);
64 plot(t1,S(:,166)), axis([106 306 -3 3])
65 grid on
66 title('Received signal at {\alpha} = 75{^{\circ}} ')
67 xlabel('t ({\mu}s)')
68 ylabel('Voltage (V)')
69
70
71
72
73
74 hold off
75
76 figure(5),
77 subplot(3,2,1);
78 plot(t1,S(:,176)), axis([106 306 -3 3])
79 grid on
80 title('Received signal at {\alpha} = 85{^{\circ}} ')
81 xlabel('t ({\mu}s)')
82 ylabel('Voltage (V)')
83
84 subplot(3,2,2);
85 plot(t1,S(:,177)), axis([106 306 -3 3])
86 grid on
87 title('Received signal at {\alpha} = 86{^{\circ}} ')
88 xlabel('t ({\mu}s)')
```

```
ylabel('Voltage (V)')

subplot(3,2,3);
plot(t1,S(:,178)), axis([106 306 -3 3])
grid on
title('Received signal at {\alpha} = 87{^{\circ}} ' )
xlabel('t ({\mu}s)')
ylabel('Voltage (V)')

subplot(3,2,4);
plot(t1,S(:,179)), axis([106 306 -3 3])
grid on
title('Received signal at {\alpha} = 88{^{\circ}} ' )
xlabel('t ({\mu}s)')
ylabel('Voltage (V)')

subplot(3,2,5);
plot(t1,S(:,180)), axis([106 306 -3 3])
grid on
title('Received signal at {\alpha} = 89{^{\circ}} ' )
xlabel('t ({\mu}s)')
ylabel('Voltage (V)')

subplot(3,2,6);
plot(t1,S(:,181)), axis([106 306 -3 3])
grid on
title('Received signal at {\alpha} = 90{^{\circ}} ' )
xlabel('t ({\mu}s)')
ylabel('Voltage (V)')

figure(6),

imagesc(angle,t1,db(S/max(S(:))));
colorbar;
title('Decibel of the signals')
ylabel('Time, {\mu}s');
xlabel('Rotational angle, {\alpha}');
```

Beampattern code for Chapter 8:

```
load('exp_front181p_d21_4cm_Vpp.mat')

r = 6E-2;
x0 = 21.4E-2;

L = 0.01;
L1 = 0.011; L2 = 0.012; L3 = 0.013; L4 = 0.014; L5 =
    0.015; L6=0.016;
```

```
lambda = 0.01488;

alpha = [-pi/2:pi/180:pi/2];
a = r.*sin(alpha);
b = r.*cos(alpha);
b_p = r - b;
x_p = x0 + b_p;
x = sqrt((a.^2) + (x_p.^2));
phi = asin(a./x);

theta_p = alpha + phi;


s = ((sin((pi*L/lambda).*sin(theta_p))./((pi*L/lambda
    ).*sin(theta_p)));
s2 = ((sin((pi*L/lambda).*sin(theta_p))./((pi/lambda)
    .*sin(theta_p)));
%plot(theta, b)

figure(1);
g1 = plot(theta_p, db(s),'m')


hold on
g2 = plot(theta_p, db(s2/max(s2)),'o')

axis([-pi/2 pi/2 -15 0])
title('Decibel value of the amplitude w/d=1cm.')
xlabel('Beam Angle, {\theta_{p}} in radians')
ylabel('Normalized Amplitude, dBV')
grid on


S = ((sin((pi*L/lambda).*sin(theta_p))./((pi*L/lambda
    ).*sin(theta_p))).*cos(theta_p);

g4 = plot(theta_p, db(S), 'g')

S1 = ((sin((pi*L/lambda).*sin(theta_p))./((pi*L/
    lambda).*sin(theta_p))).*((1+cos(theta_p))./2);

g5 = plot(theta_p, db(S1), 'k')
g3 = plot(theta_p,smooth(db(Vpp/max(Vpp))),'r')

 h = legend('$\frac{sin[(\pi d/\lambda)\times sin(\
    theta_{p})]}{(\pi d/\lambda)\times sin(\theta_{p})
    }$','$\frac{sin[(k_x d/2)]}{(k_x/2)}$', '$\frac{
    sin[(\pi d/\lambda)\times sin(\theta_{p})]}{(\pi d
```

```
      /\lambda)\times sin(\theta_{p})}\times cos(\theta_
      {p})$','$\frac{sin[(\pi d/\lambda)\times sin(\
      theta_{p})]}{(\pi d/\lambda)\times sin(\theta_{p})
      }\times \frac{1+cos(\theta_{p})}{2}$','Meassured
      Amplitude');
49    set(h,'Interpreter','latex')
50    set(gca,'fontsize',10)
51
52    set(g1, 'linewidth', 2);
53    set(g2, 'linewidth', 2);
54    set(g3, 'linewidth', 2);
55    set(g4, 'linewidth', 2);
56    set(g5, 'linewidth', 2);
57
58
59
60    s_1 = ((sin((pi*L1/lambda).*sin(theta_p))./((pi*L1/
        lambda).*sin(theta_p)));
61  s2_1 = ((sin((pi*L1/lambda).*sin(theta_p))./((pi/
      lambda).*sin(theta_p)));
62  S_1 = ((sin((pi*L1/lambda).*sin(theta_p))./((pi*L1/
      lambda).*sin(theta_p))).*cos(theta_p);
63  S1_1 = ((sin((pi*L1/lambda).*sin(theta_p))./((pi*L1/
      lambda).*sin(theta_p))).*((1+cos(theta_p))./2);
64
65  figure(2);
66  subplot(3,2,1);
67  g1_1 = plot(theta_p, db(s_1),'m')
68
69
70  hold on
71  g2_1 = plot(theta_p, db(s2_1/max(s2_1)),'o')
72
73  axis([-pi/2 pi/2 -15 0])
74  title('Decibel value of the amplitude w/d=1.1cm.')
75  xlabel('Beam Angle, {\theta_{p}} in radians')
76  ylabel('Normalized Amplitude, dBV')
77  grid on
78
79  g4_1 = plot(theta_p, db(S_1), 'g')
80
81  g5_1 = plot(theta_p, db(S1_1), 'k')
82  g3_1 = plot(theta_p,smooth(db(Vpp/max(Vpp))),'r')
83
84  %  h1 =legend('$\frac{sin[(\pi d/\lambda)\times sin(\
      theta_{p})]}{(\pi d/\lambda)\times sin(\theta_{p})}
      $','$\frac{sin[(k_x d/2)]}{(k_x/2)}$', '$\frac{sin
      [(\pi d/\lambda)\times sin(\theta_{p})]}{(\pi d/\
```

```
    lambda)\times sin(\theta_{p})}\times cos(\theta_{p
    })$','$\frac{sin[(\pi d/\lambda)\times sin(\theta_{
    p})]}{(\pi d/\lambda)\times sin(\theta_{p})}\times
    \frac{1+cos(\theta_{p})}{2}$','Meassured Amplitude
    ');
%   set(h1,'Interpreter','latex')
%    set(gca,'fontsize',10)

  set(g1_1, 'linewidth', 2);
  set(g2_1, 'linewidth', 2);
  set(g3_1, 'linewidth', 2);
  set(g4_1, 'linewidth', 2);
  set(g5_1, 'linewidth', 2);



   s_2 = ((sin((pi*L2/lambda).*sin(theta_p))./((pi*L2
      /lambda).*sin(theta_p)));
s2_2 = ((sin((pi*L2/lambda).*sin(theta_p))./((pi/
    lambda).*sin(theta_p)));
S_2 = ((sin((pi*L2/lambda).*sin(theta_p))./((pi*L2/
    lambda).*sin(theta_p))).*cos(theta_p);
S1_2 = ((sin((pi*L2/lambda).*sin(theta_p))./((pi*L2/
    lambda).*sin(theta_p))).*((1+cos(theta_p))./2);
  subplot(3,2,2);
g1_2 = plot(theta_p, db(s_2),'m')


hold on
g2_2 = plot(theta_p, db(s2_2/max(s2_2)),'o')

axis([-pi/2 pi/2 -15 0])
title('Decibel value of the amplitude w/d=1.2cm.')
xlabel('Beam Angle, {\theta_{p}} in radians')
ylabel('Normalized Amplitude, dBV')
grid on

g4_2 = plot(theta_p, db(S_2), 'g')

g5_2 = plot(theta_p, db(S1_2), 'k')

g3_2 = plot(theta_p,smooth(db(Vpp/max(Vpp))),'r')

  set(g1_2, 'linewidth', 2);
  set(g2_2, 'linewidth', 2);
  set(g3_2, 'linewidth', 2);
  set(g4_2, 'linewidth', 2);
  set(g5_2, 'linewidth', 2);
```

```
124
125       s_3 = ((sin((pi*L3/lambda).*sin(theta_p))./((pi*
              L3/lambda).*sin(theta_p)));
126 s2_3 = ((sin((pi*L3/lambda).*sin(theta_p))./((pi/
          lambda).*sin(theta_p)));
127 S_3 = ((sin((pi*L3/lambda).*sin(theta_p))./((pi*L3/
          lambda).*sin(theta_p))).*cos(theta_p);
128 S1_3 = ((sin((pi*L3/lambda).*sin(theta_p))./((pi*L3/
          lambda).*sin(theta_p))).*((1+cos(theta_p))./2);
129   subplot(3,2,3);
130 g1_3 = plot(theta_p, db(s_3),'m')
131
132
133 hold on
134 g2_3 = plot(theta_p, db(s2_3/max(s2_3)),'o')
135
136 axis([-pi/2 pi/2 -15 0])
137 title('Decibel value of the amplitude w/d=1.3cm.')
138 xlabel('Beam Angle, {\theta_{p}} in radians')
139 ylabel('Normalized Amplitude, dBV')
140 grid on
141
142 g4_3 = plot(theta_p, db(S_3), 'g')
143
144 g5_3 = plot(theta_p, db(S1_3), 'k')
145
146 g3_3 = plot(theta_p,smooth(db(Vpp/max(Vpp))),'r')
147
148   set(g1_3, 'linewidth', 2);
149   set(g2_3, 'linewidth', 2);
150   set(g3_3, 'linewidth', 2);
151   set(g4_3, 'linewidth', 2);
152   set(g5_3, 'linewidth', 2);
153
154    s_4 = ((sin((pi*L4/lambda).*sin(theta_p))./((pi*L4
             /lambda).*sin(theta_p)));
155 s2_4 = ((sin((pi*L4/lambda).*sin(theta_p))./((pi/
          lambda).*sin(theta_p)));
156 S_4 = ((sin((pi*L4/lambda).*sin(theta_p))./((pi*L4/
          lambda).*sin(theta_p))).*cos(theta_p);
157 S1_4 = ((sin((pi*L4/lambda).*sin(theta_p))./((pi*L4/
          lambda).*sin(theta_p))).*((1+cos(theta_p))./2);
158   subplot(3,2,4);
159 g1_4 = plot(theta_p, db(s_4),'m')
160
161
162 hold on
163 g2_4 = plot(theta_p, db(s2_4/max(s2_4)),'o')
```

```
164
165 axis([-pi/2 pi/2 -15 0])
166 title('Decibel value of the amplitude w/d=1.4cm.')
167 xlabel('Beam Angle, {\theta_{p}} in radians')
168 ylabel('Normalized Amplitude, dBV')
169 grid on
170
171 g4_4 = plot(theta_p, db(S_4), 'g')
172
173 g5_4 = plot(theta_p, db(S1_4), 'k')
174
175 g3_4 = plot(theta_p,smooth(db(Vpp/max(Vpp))),'r')
176
177   set(g1_4, 'linewidth', 2);
178   set(g2_4, 'linewidth', 2);
179   set(g3_4, 'linewidth', 2);
180   set(g4_4, 'linewidth', 2);
181   set(g5_4, 'linewidth', 2);
182
183    s_5 = ((sin((pi*L5/lambda).*sin(theta_p))./((pi*L5
        /lambda).*sin(theta_p)));
184 s2_5 = ((sin((pi*L5/lambda).*sin(theta_p))./((pi/
    lambda).*sin(theta_p)));
185 S_5 = ((sin((pi*L5/lambda).*sin(theta_p))./((pi*L5/
    lambda).*sin(theta_p))).*cos(theta_p);
186 S1_5 = ((sin((pi*L5/lambda).*sin(theta_p))./((pi*L5/
    lambda).*sin(theta_p))).*((1+cos(theta_p))./2);
187   subplot(3,2,5);
188 g1_5 = plot(theta_p, db(s_5),'m')
189
190
191 hold on
192 g2_5 = plot(theta_p, db(s2_5/max(s2_5)),'o')
193
194 axis([-pi/2 pi/2 -15 0])
195 title('Decibel value of the amplitude w/d=1.5cm.')
196 xlabel('Beam Angle, {\theta_{p}} in radians')
197 ylabel('Normalized Amplitude, dBV')
198 grid on
199
200 g4_5 = plot(theta_p, db(S_5), 'g')
201
202 g5_5 = plot(theta_p, db(S1_5), 'k')
203
204 g3_5 = plot(theta_p,smooth(db(Vpp/max(Vpp))),'r')
205
206   set(g1_5, 'linewidth', 2);
207   set(g2_5, 'linewidth', 2);
```

```
208   set(g3_5, 'linewidth', 2);
209   set(g4_5, 'linewidth', 2);
210   set(g5_5, 'linewidth', 2);
211
212       s_6 = ((sin((pi*L6/lambda).*sin(theta_p))./((pi*
          L6/lambda).*sin(theta_p)));
213 s2_6 = ((sin((pi*L6/lambda).*sin(theta_p))./((pi/
    lambda).*sin(theta_p)));
214 S_6 = ((sin((pi*L6/lambda).*sin(theta_p))./((pi*L6/
    lambda).*sin(theta_p))).*cos(theta_p);
215 S1_6 = ((sin((pi*L6/lambda).*sin(theta_p))./((pi*L6/
    lambda).*sin(theta_p))).*((1+cos(theta_p))./2);
216   subplot(3,2,6);
217 g1_6 = plot(theta_p, db(s_6),'m')
218
219
220 hold on
221 g2_6 = plot(theta_p, db(s2_6/max(s2_6)),'o')
222
223 axis([-pi/2 pi/2 -15 0])
224 title('Decibel value of the amplitude w/d=1.6cm.')
225 xlabel('Beam Angle, {\theta_{p}} in radians')
226 ylabel('Normalized Amplitude, dBV')
227 grid on
228
229 g4_6 = plot(theta_p, db(S_6), 'g')
230
231 g5_6 = plot(theta_p, db(S1_6), 'k')
232
233 g3_6 = plot(theta_p,smooth(db(Vpp/max(Vpp))),'r')
234
235   set(g1_6, 'linewidth', 2);
236   set(g2_6, 'linewidth', 2);
237   set(g3_6, 'linewidth', 2);
238   set(g4_6, 'linewidth', 2);
239   set(g5_6, 'linewidth', 2);
```

Code for experiemnt IV:

```
1 load('exp_back_85to275_2.mat')
2 load('exp_back_85to275_Vpp_2.mat')
3
4 t = [78:0.5:577.5];
5 angle = [85:1:275];
6
7
8 figure(1),plot(t,S)
9 axis([78 578 -1 1])
```

```
grid on
title('Measurements for rotational angle {\alpha} {\in} [-90{^{\circ}}, 90{^{\circ}}]. ')
xlabel('t ({\mu}s)')
ylabel('Voltage (V)')

figure(2),plot(angle,smooth((Vpp)),'r')
axis([85 275 0 1.3])
title('Amplitude plot')
xlabel('Rotational Angle, {\alpha}')
ylabel('Normalized Amplitude, dBV')
grid on


figure(3);
subplot(3,2,1);
plot(t,S(:,1)), axis([78 578 -0.6 0.6])
grid on
title('Received signal at {\alpha} = 85{^{\circ}} ')
xlabel('t ({\mu}s)')
ylabel('Voltage (V)')

subplot(3,2,2);
plot(t,S(:,2)), axis([78 578 -0.6 0.6])
grid on
title('Received signal at {\alpha} = 86{^{\circ}} ')
xlabel('t ({\mu}s)')
ylabel('Voltage (V)')

subplot(3,2,3);
plot(t,S(:,3)), axis([78 578 -0.6 0.6])
grid on
title('Received signal at {\alpha} = 87{^{\circ}} ')
xlabel('t ({\mu}s)')
ylabel('Voltage (V)')

subplot(3,2,4);
plot(t,S(:,4)), axis([78 578 -0.6 0.6])
grid on
title('Received signal at {\alpha} = 88{^{\circ}} ')
xlabel('t ({\mu}s)')
ylabel('Voltage (V)')

subplot(3,2,5);
plot(t,S(:,5)), axis([78 578 -0.6 0.6])
grid on
title('Received signal at {\alpha} = 89{^{\circ}} ')
xlabel('t ({\mu}s)')
```

```
57 ylabel('Voltage (V)')
58
59 subplot(3,2,6);
60 plot(t,S(:,6)), axis([78 578 -0.6 0.6])
61 grid on
62 title('Received signal at {\alpha} = 90{^{\circ}} ' )
63 xlabel('t ({\mu}s)')
64 ylabel('Voltage (V)')
65
66
67 figure(4), subplot(5,3,1);
68 plot(t,S(:,1)), axis([78 578 -0.6 0.6])
69 grid on
70 title('Received signal at {\alpha} = 85{^{\circ}} ' )
71 xlabel('t ({\mu}s)')
72 ylabel('Voltage (V)')
73
74 subplot(5,3,2);
75 plot(t,S(:,6)), axis([78 578 -0.6 0.6])
76 grid on
77 title('Received signal at {\alpha} = 90{^{\circ}} ' )
78 xlabel('t ({\mu}s)')
79 ylabel('Voltage (V)')
80
81 subplot(5,3,3);
82 plot(t,S(:,26)), axis([78 578 -0.6 0.6])
83 grid on
84 title('Received signal at {\alpha} = 110{^{\circ}} ' )
85 xlabel('t ({\mu}s)')
86 ylabel('Voltage (V)')
87
88 subplot(5,3,4);
89 plot(t,S(:,36)), axis([78 578 -0.6 0.6])
90 grid on
91 title('Received signal at {\alpha} = 120{^{\circ}} ' )
92 xlabel('t ({\mu}s)')
93 ylabel('Voltage (V)')
94
95 subplot(5,3,5);
96 plot(t,S(:,61)), axis([78 578 -0.6 0.6])
97 grid on
98 title('Received signal at {\alpha} = 145{^{\circ}} ' )
99 xlabel('t ({\mu}s)')
100 ylabel('Voltage (V)')
101
102 subplot(5,3,6);
103 plot(t,S(:,76)), axis([78 578 -0.6 0.6])
104 grid on
```

```
105 title('Received signal at {\alpha} = 160{^{\circ}} ')
106 xlabel('t ({\mu}s)')
107 ylabel('Voltage (V)')
108
109 subplot(5,3,7);
110 plot(t,S(:,95)), axis([78 578 -0.6 0.6])
111 grid on
112 title('Received signal at {\alpha} = 179{^{\circ}} ')
113 xlabel('t ({\mu}s)')
114 ylabel('Voltage (V)')
115
116 subplot(5,3,8);
117 plot(t,S(:,96)), axis([78 578 -0.6 0.6])
118 grid on
119 title('Received signal at {\alpha} = 180{^{\circ}} ')
120 xlabel('t ({\mu}s)')
121 ylabel('Voltage (V)')
122
123 subplot(5,3,9);
124 plot(t,S(:,97)), axis([78 578 -0.6 0.6])
125 grid on
126 title('Received signal at {\alpha} = 181{^{\circ}} ')
127 xlabel('t ({\mu}s)')
128 ylabel('Voltage (V)')
129
130 subplot(5,3,10);
131 plot(t,S(:,116)), axis([78 578 -0.6 0.6])
132 grid on
133 title('Received signal at {\alpha} = 200{^{\circ}} ')
134 xlabel('t ({\mu}s)')
135 ylabel('Voltage (V)')
136
137 subplot(5,3,11);
138 plot(t,S(:,131)), axis([78 578 -0.6 0.6])
139 grid on
140 title('Received signal at {\alpha} = 215{^{\circ}} ')
141 xlabel('t ({\mu}s)')
142 ylabel('Voltage (V)')
143
144 subplot(5,3,12);
145 plot(t,S(:,156)), axis([78 578 -0.6 0.6])
146 grid on
147 title('Received signal at {\alpha} = 240{^{\circ}} ')
148 xlabel('t ({\mu}s)')
149 ylabel('Voltage (V)')
150
151 subplot(5,3,13);
152 plot(t,S(:,166)), axis([78 578 -0.6 0.6])
```

```
153 grid on
154 title('Received signal at {\alpha} = 250{^{\circ}} ')
155 xlabel('t ({\mu}s)')
156 ylabel('Voltage (V)')
157
158 subplot(5,3,14);
159 plot(t,S(:,186)), axis([78 578 -0.6 0.6])
160 grid on
161 title('Received signal at {\alpha} = 270{^{\circ}} ')
162 xlabel('t ({\mu}s)')
163 ylabel('Voltage (V)')
164
165 subplot(5,3,15);
166 plot(t,S(:,191)), axis([78 578 -0.6 0.6])
167 grid on
168 title('Received signal at {\alpha} = 275{^{\circ}} ')
169 xlabel('t ({\mu}s)')
170 ylabel('Voltage (V)')
171
172 figure(5);
173 subplot(3,2,1);
174 plot(t,S(:,11)), axis([78 578 -0.6 0.6])
175 grid on
176 title('Received signal at {\alpha} = 95{^{\circ}} ')
177 xlabel('t ({\mu}s)')
178 ylabel('Voltage (V)')
179
180 subplot(3,2,2);
181 plot(t,S(:,16)), axis([78 578 -0.6 0.6])
182 grid on
183 title('Received signal at {\alpha} = 100{^{\circ}} ')
184 xlabel('t ({\mu}s)')
185 ylabel('Voltage (V)')
186
187 subplot(3,2,3);
188 plot(t,S(:,21)), axis([78 578 -0.6 0.6])
189 grid on
190 title('Received signal at {\alpha} = 105{^{\circ}} ')
191 xlabel('t ({\mu}s)')
192 ylabel('Voltage (V)')
193
194 subplot(3,2,4);
195 plot(t,S(:,26)), axis([78 578 -0.6 0.6])
196 grid on
197 title('Received signal at {\alpha} = 110{^{\circ}} ')
198 xlabel('t ({\mu}s)')
199 ylabel('Voltage (V)')
200
```

```
subplot(3,2,5);
plot(t,S(:,31)), axis([78 578 -0.6 0.6])
grid on
title('Received signal at {\alpha} = 115{^{\circ}} ')
xlabel('t ({\mu}s)')
ylabel('Voltage (V)')

subplot(3,2,6);
plot(t,S(:,36)), axis([78 578 -0.6 0.6])
grid on
title('Received signal at {\alpha} = 120{^{\circ}} ')
xlabel('t ({\mu}s)')
ylabel('Voltage (V)')


figure(6)
plot(angle, db(smooth(Vpp)));
axis([85 275 -50 5.5])
grid on
title('Amplitude plot in dB')
ylabel('Amplitude, dBV');
xlabel('Rotational angle, {\alpha}');

figure(7)
imagesc(angle,t,db(S/max(S(:))));
colorbar;
title('Decibel of the signals')
ylabel('Time, {\mu}s');
xlabel('Rotational angle, {\alpha}');


load('exp_front181p_d21_4cm_Vpp.mat');
Vpp_1 = Vpp(91:181);
Vpp_2 = Vpp(1:90);

load('exp_back_85to275_Vpp_2.mat');
Vpp_3 = Vpp(1:96);
Vpp_4 = Vpp(97:191);

angle1 = [0:1:90]; angle2 = [270:1:359]; angle3 =
   [85:1:180]; angle4 = [181:1:275];

figure(1);
plot(angle1, (Vpp_1));
hold on
plot(angle2, (Vpp_2), 'r');
plot(angle3, (Vpp_3), 'g');
plot(angle4, (Vpp_4), 'k');
```

```
18 axis([0 359 0 6])
19 title('Amplitude of experiments III and IV')
20 xlabel('Rotational Angle, {\alpha}')
21 ylabel('Amplitude, V')
22 legend('Experiment III [0{^{\circ}} - 90{^{\circ}}]',
       'Experiment III [270{^{\circ}} - 359{^{\circ}}]','
       Experiment IV [85{^{\circ}} - 180{^{\circ}}]', '
       Experiment IV [181{^{\circ}} - 275{^{\circ}}]')
23 grid on
24
25 figure(2);
26 Vpp1_1 = Vpp_1(1:86) + (Vpp_3(1) - Vpp_1(86));
27 Vpp2_1 = Vpp_2(6:90) - (Vpp_2(6) - Vpp_4(95));
28 Vpp3_1 = Vpp_3(1:96);
29 Vpp4_1 = Vpp_4(1:95);
30
31 angle1_1 = [0:1:85]; angle2_2 = [275:1:359];
32
33 plot(angle1_1, smooth(Vpp1_1));
34 hold on
35 plot(angle2_2, smooth(Vpp2_1), 'r');
36 plot(angle3, smooth(Vpp3_1), 'k');
37 plot(angle4, smooth(Vpp4_1), 'g');
38 axis([0 359 0 6])
39 title('Compensated Amplitude of experiments III and IV
       ')
40 xlabel('Rotational Angle, {\alpha}')
41 ylabel('Amplitude, V')
42 legend('Experiment III [0{^{\circ}} - 90{^{\circ}}]',
       'Experiment III [270{^{\circ}} - 359{^{\circ}}]','
       Experiment IV [85{^{\circ}} - 180{^{\circ}}]', '
       Experiment IV [181{^{\circ}} - 275{^{\circ}}]')
43 grid on
44
45 figure(3);
46 plot(angle1_1, db(smooth(Vpp1_1)));
47 hold on
48 plot(angle2_2, db(smooth(Vpp2_1)), 'r');
49 plot(angle3, db(smooth(Vpp3_1)), 'k');
50 plot(angle4, db(smooth(Vpp4_1)), 'g');
51 title('Compensated Amplitude in dB of experiments III
       and IV')
52 xlabel('Rotational Angle, {\alpha}')
53 ylabel('Amplitude, dBV')
54 legend('Experiment III [0{^{\circ}} - 90{^{\circ}}]',
       'Experiment III [270{^{\circ}} - 359{^{\circ}}]','
       Experiment IV [85{^{\circ}} - 180{^{\circ}}]', '
       Experiment IV [181{^{\circ}} - 275{^{\circ}}]')
```

```
55 grid on
56 axis([0 359 -55 16])
57
58 figure(4);
59 plot(angle1, db(Vpp_1));
60 hold on
61 plot(angle2, db(Vpp_2), 'r');
62 plot(angle3, db(Vpp_3), 'g');
63 plot(angle4, db(Vpp_4), 'k');
```

Bibliography

[1] *The sonar equation*. http://www.sal2000.com/ds/ds3/Acoustics/Introduction%20To%20The%20Sonar%20Equations.htm. [Online; accessed 10-August-2014].

[2] D.R. Campbell. Effect of ear separation and the human head. http://media.paisley.ac.uk/~campbell/AASP/Human%20Head.PDF, cited July 2008.

[3] Paul D Coleman. An analysis of cues to auditory depth perception in free space. *Psychological Bulletin*, 60(3):302, 1963.

[4] Zachary A Constan and William M Hartmann. On the detection of dispersion in the head-related transfer function. *The Journal of the Acoustical Society of America*, 114(2):998–1008, 2003.

[5] Richard O Duda and William L Martens. Range dependence of the response of a spherical head model. *The Journal of the Acoustical Society of America*, 104(5):3048–3058, 1998.

[6] Wikipedia, The Free Encyclopedia. *Hearing range*. http://en.wikipedia.org/wiki/Hearing_range, 2014. [Online; accessed 4th-September-2014].

[7] Wikipedia, The Free Encyclopedia. *Human head*. http://en.wikipedia.org/wiki/Human_head, 2014. [Online; accessed 4th-September-2014].

[8] Wikipedia, The Free Encyclopedia. *Sonar*. http://en.wikipedia.org/wiki/Sonar, 2014. [Online; accessed 23-July-2014].

[9] FH Fisher and VP Simmons. Sound absorption in sea water. *The Journal of the Acoustical Society of America*, 62(3):558–564, 1977.

[10] Roy Edgar Hansen. Introduction to sonar. *Course materiel to INFGEO4310*, 2009.

[11] Monson H Hayes. *Statistical digital signal processing and modelling*. John Wiley & Sons, Inc., 1996.

[12] Don H Johnson and Dudgeon Dan E. *Array signal processing: concepts and techniques*. P T R Prentice-Hall, Inc., 1993.

[13] John C Middlebrooks and David M Green. Sound localization by human listeners. *Annual review of psychology*, 42(1):135–159, 1991.

[14] Philip M Morse and K Ingard. Uno: Theoretical acoustics, 1968.

[15] Discovery of sound in the sea. *Cylindrical vs. spherical spreading*. http://www.dosits.org/science/advancedtopics/spreading/. [Online; accessed 01-August-2014].

[16] AR Selfridge, GS Kino, and BT Khuri-Yakub. A theory for the radiation pattern of a narrow-strip acoustic transducer. *Applied Physics Letters*, 37(1):35–36, 1980.

[17] Robert J Urick. *Principles of underwater sound*. McGraw-Hill, New York. US, third edition, 1983.